

MATHEMATICS MAGAZINE



- Communicating while playing with fireworks
- Fairly dividing discrete objects
- Tracing paths of foci
- An interview with George Hart

EDITORIAL POLICY

Mathematics Magazine aims to provide lively and appealing mathematical exposition. The *Magazine* is not a research journal, so the terse style appropriate for such a journal (lemma-theorem-proof-corollary) is not appropriate for the *Magazine*. Articles should include examples, applications, historical background, and illustrations, where appropriate. They should be attractive and accessible to undergraduates and would, ideally, be helpful in supplementing undergraduate courses or in stimulating student investigations. Manuscripts on history are especially welcome, as are those showing relationships among various branches of mathematics and between mathematics and other disciplines.

Submissions of articles are required via the *Mathematics Magazine's* Editorial Manager System. The name(s) of the author(s) should not appear in the file. Initial submissions in pdf or LaTeX form can be sent to the editor at www.editorialmanager.com/mathmag/.

The Editorial Manager System will cue the author for all required information concerning the paper. Questions concerning submission of papers can be addressed to the editor at mathmag@maa.org. Authors who use LaTeX are urged to use the *Magazine* article template. However, a LaTeX file that uses a generic article class with no custom formatting is acceptable. The template and the Guidelines for Authors can be downloaded from www.maa.org/pubs/mathmag.

MATHEMATICS MAGAZINE (ISSN 0025-570X) is published by the Mathematical Association of America at 1529 Eighteenth Street, NW, Washington, DC 20036 and Lancaster, PA, in the months of February, April, June, October, and December.

Microfilmed issues may be obtained from University Microfilms International, Serials Bid Coordinator, 300 North Zeeb Road, Ann Arbor, MI 48106.

Address advertising correspondence to

MAA Advertising
1529 Eighteenth St. NW
Washington, DC 20036
Phone: (202) 319-8461
E-mail: advertising@maa.org

Further advertising information can be found online at www.maa.org.

Change of address, missing issue inquiries, and other subscription correspondence can be sent to:

The MAA Customer Service Center
P.O. Box 91112
Washington, DC 20090-1112
(800) 331-1622
(301) 617-7800
maaservice@maa.org

Copyright © by the Mathematical Association of America (Incorporated), 2015, including rights to this journal issue as a whole and, except where otherwise noted, rights to each individual contribution. Permission to make copies of individual articles, in paper or electronic form, including posting on personal and class web pages, for educational and scientific use is granted without fee provided that copies are not made or distributed for profit or commercial advantage and that copies bear the following copyright notice:

Copyright the Mathematical Association of America 2015. All rights reserved.

Abstracting with credit is permitted. To copy otherwise, or to republish, requires specific permission of the MAA's Director of Publication and possibly a fee.

Periodicals postage paid at Washington, D.C. and additional mailing offices.

Postmaster: Send address changes to Membership/Subscriptions Department, Mathematical Association of America, 1529 Eighteenth Street, NW, Washington, DC 20036-1385.

Printed in the United States of America.

COVER IMAGE

Hanabi © 2016 David A. Reimann (*Albion College*). Used by permission.

The fireworks display uses the digits 1–5 for the embers in the fireworks, corresponding to the numbers on the cards in the game *Hanabi*. The article “How to Make the Perfect Fireworks Display: Two Strategies for *Hanabi*” by Cox et al. was the inspiration for this piece.

MATHEMATICS MAGAZINE

EDITOR

Michael A. Jones
Mathematical Reviews

ASSOCIATE EDITORS

Bernardo M. Ábrego
California State University - Northridge

Julie C. Beier
Earlham College

Leah W. Berman
University of Alaska - Fairbanks

Paul J. Campbell
Beloit College

Annalisa Crannell
Franklin & Marshall College

Stephanie Edwards
Hope College

Rebecca Garcia
Sam Houston State University

James D. Harper
Central Washington University

Deanna B. Haunsperger
Carleton College

Allison K. Henrich
Seattle University

Warren P. Johnson
Connecticut College

Keith M. Kendig
Cleveland State University

Dawn A. Lott
Delaware State University

Jane McDougall
Colorado College

Anthony Mendes
California Polytechnic State University

Lon Mitchell
Mathematical Reviews

Roger B. Nelsen
Lewis & Clark College

David R. Scott
University of Puget Sound

Brittany Shelton
Albright College

Paul K. Stockmeyer
College of William & Mary

Jennifer M. Wilson
Eugene Lang College
The New School

MANAGING EDITOR

Beverly Joy Ruedi

ASSISTANT MANAGING EDITOR

Bonnie K. Ponce

LETTER FROM THE EDITOR

The lead article in this issue is *How to Make the Perfect Fireworks Display: Two Strategies for Hanabi* by Christopher Cox, Jessica De Silva, Philip DeOrsey, Franklin H. J. Kenter, Troy Retter, and Josh Tobin. This manuscript, which was also the inspiration for David Reimann's art on the cover of this issue, describes a way in which players can communicate to achieve better outcomes in the card game *Hanabi*. The mathematics is motivated by hat-guessing games.

Steven Brams, Marc Kilgour, and Christian Klamler offer an article on how to divide things fairly. They propose a simple algorithm to allocate discrete "things," and then analyze the outcome by considering whether the outcome always satisfies certain fairness criteria.

In *Volume/Surface Area Ratios for Globes, with Applications*, Tom Apostol and Mamikon Mnatsakanian compute some surprising ratios between volumes and surface areas, and between surface areas and volumes, for a collection of different solids of revolution. For those familiar with the work of Apostol and Mnatsakanian, the article includes an abundance of helpful figures.

Impeccable drawings also play an important part of *Foci Loci and Toric Sections* by Michael Gaul and Fred Kuczmarski. They investigate the curves, named foci loci, traced by the foci of one-parameter families of ellipses. How does the torus make an appearance? As suggested by the title, these focal paths end up being the cross sections of tori.

This issue includes the first of what is expected to be a series of interviews with mathematical artists or artistic mathematicians. Amy and David Reimann spoke to George Hart and a portion of their conversation appears in this issue as *George Hart: Troubadour for Geometry*.

Mixed in are two proofs without words, one by Grégoire Nicollier and the other by Angel Plaza, as well as a few filler items, including an identity to welcome in 2016. Additionally, sprinkled throughout the issue are images of George Hart's artwork that accompany the interview article.

Brendan Sullivan provides a crossword with a theme of the 2016 Joint Mathematics Meetings (JMM). As this issue of the *MAGAZINE* will not go to press until after the Joint Meetings, the MAA tweeted some of the clues and they posted the crossword on the MAA homepage (including in the .puz format that many solvers use). Additionally, paper copies of the crossword were available at the MAA booth at the meetings. I hope that Brendan will make this the first annual crossword tied to the JMM.

As per usual, this issue includes the Problems section. However, let me take this opportunity to announce some changes on the *MAGAZINE*'s editorial board as it relates to the Problems section. This is the last issue in which Bernardo Àbrego is serving as the Problems Editor. Bernardo has been the Problems Editor for six years, or 30 issues. During that time, Bernardo and the associate editors of the Problems section have prepared for publication 150 problems and accompanying solutions, as well as the quickies. The Problems section is one of the most popular features for each of the MAA journals. I thank Bernardo and Bernardo's colleagues Silvia Fernández-Merchant and William Watkins, who will also be stepping down from serving on the Problems editorial board, for their service and for their contributions in making *MATHEMATICS MAGAZINE* a pleasure to read. With this "goodbye" comes a "hello," as I would like to welcome Eduardo Dueñez of the University of Texas at San Antonio to the position as Problems Editor. I'll welcome him more fully in the February issue.

Finally, the issue concludes with the Reviews section, which includes a review of Lynn Gamwell's *Mathematics and Art: A Cultural History*. Two proofreaders of the Reviews section have already bought this book based on reading the review! Check out the rest of the Reviews to get an idea of what else to read.

Michael A. Jones, Editor

ARTICLES

How to Make the Perfect Fireworks Display: Two Strategies for *Hanabi*

CHRISTOPHER COX

Carnegie Mellon University
Pittsburgh, PA 15213
cocox@andrew.cmu.edu

JESSICA DE SILVA

University of Nebraska-Lincoln
Lincoln, NE 68508
jessica.desilva@huskers.unl.edu

PHILIP DEORSEY

Emory & Henry College
Emory, VA 24327
pdeorsey@ehc.edu

FRANKLIN H. J. KENTER

Rice University
Houston, TX 77005
franklin.h.kenter@rice.edu

TROY RETTER

Emory University
Atlanta, GA 30322
tretter@emory.edu

JOSH TOBIN

University of California, San Diego
La Jolla, CA 92093
rjtobin@ucsd.edu

Hanabi is a card game by Antoine Bruza which won the prestigious *Spiel des Jahres* (Game of the Year) in 2013 [10]. Named after the Japanese word for fireworks, the game is based upon creating the perfect fireworks display by playing cards, i.e. fireworks, in a desirable sequence. Unlike conventional card games, players see cards in other players' hands but not their own and work together as a team. Hence, game-play is focused on the players discovering information about their own cards through the limited communication the game allows. Only through clever strategy, coordinated implementation, and a bit of luck can the team successfully create the perfect fireworks display.

In order to devise a strategy for *Hanabi* in which players communicate information effectively, we turn to *hat guessing games* for inspiration. Hat guessing games are a popular topic in recreational mathematics [3, 4, 5, 7, 8, 11]. Consider the following version of a hat guessing game. Five people each put on either a red or blue hat at random and stand so that each person can see the color of every other person's hat but

not their own. If the people guess the color of their own hats sequentially out loud, how can they maximize the expected number of correct guesses? By guessing randomly, on average only 2.5 people will guess correctly. On the other hand, by implementing a clever strategy, the players can guarantee that 4 players will always guess correctly! We will discuss such a strategy and its application to *Hanabi* in later sections.

Hat guessing games are problems that arise in coding theory. Coding theory has many real world applications in communication theory [9], and it has also been used to study other games such as Sudoku [1]. Our approach to *Hanabi* is similar to the more modern topic of *network coding*, where multiple agents with asymmetric information try to communicate effectively. For example, suppose that two people wish to communicate simultaneously via a satellite. After the satellite receives the two messages A and B , which are numbers, the satellite can then broadcast $A + B$ once instead of broadcasting the two messages in sequence. Each person can then use the message she sent along with the broadcasted message to deduce the message sent to her, i.e., $B = (A + B) - A$. As a result, the satellite becomes more efficient by broadcasting half as many messages!

This article presents two strategies for *Hanabi* that incorporate ideas from hat guessing games and network coding. These strategies work similarly to the satellite example above, where a player who is giving hints acts as the satellite and the contents of the other players' hands act as messages. In turn, each hint is more effective and hence, more fireworks are made with fewer hints.

In the first strategy, hints are used to recommend actions to players. In the second strategy, hints are used to tell the players information about their cards. Results from computer simulations demonstrate that both strategies perform well, and that the more advanced information strategy achieves a perfect score over 75 percent of the time. In comparison, this is only slightly worse than a scenario in which the players cheat by looking at their own hands and play by a simple heuristic.

This article begins with an overview of the rules of *Hanabi* followed by a discussion of the hat guessing game ideas incorporated into both of our strategies. We then describe our two strategies and conclude by discussing results of computer simulations.

Overview of the rules of *Hanabi*

Here we give a brief overview of the rules of *Hanabi*. We focus on the original variation of the game with five players although most of the concepts throughout can be adapted to other variations.

The game *Hanabi* is played with a special deck of cards, each card representing a specific firework. Each card has a *rank*, which is a number 1 through 5, and a *suit*, which is one of five colors. The deck consists of 50 cards with 10 cards in each of the five suits. Within each suit, there are three '1's, two '2's, two '3's, two '4's, and one '5'.

Each player begins with a hand of four cards which are held so that all other players can see them but she cannot. The team also begins with eight *hint tokens*. Starting with the youngest player, players take turns in the clockwise direction performing one of three actions: play a card, discard a card, or give a hint.

To play a card, a player selects a card in her hand, declares she is playing the card, and then reveals the card. The cards that have already been played are placed in piles based on suit, with the most recent, i.e., highest rank, card on top as demonstrated in Figure 1a. The new card will be successfully played if its rank is exactly one higher than the last successfully played card of the same suit and a '1' is successful if no cards of that suit have been previously played. For example, in Figure 1a the following cards

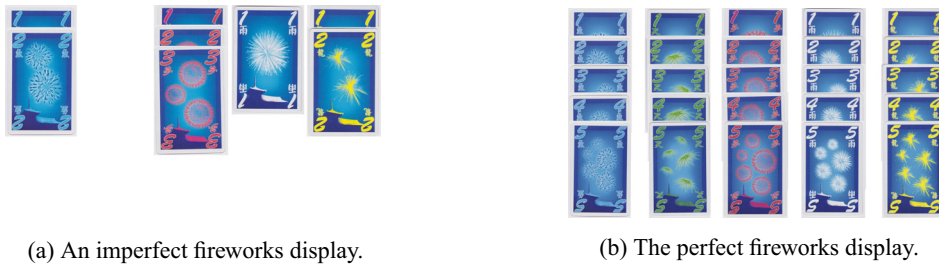


Figure 1 Examples of different fireworks displays.

can be successfully played at the current game state: blue 3, green 1, red 4, white 2, and yellow 3. If the card is successfully played, it is then added to the appropriate pile and the fireworks display becomes one firework brighter! A perfect score corresponds to a fireworks display of 25 cards as seen in Figure 1b. An unsuccessfully played card is removed from the game and the team makes an *error*; that is, the team tried to launch a firework at the wrong time. In either the event of a successful or unsuccessful play, the player draws a card if the deck is nonempty.

To discard a card, the player selects a card in her hand, declares she is discarding the card, and then reveals the card. The card is removed from the game and the team is awarded a hint token, provided the team has fewer than eight hint tokens. She then draws a card, provided the deck is not empty.

To give a hint, one player selects another player and identifies all cards in the other player's hand of a particular rank or suit, e.g., "These two cards are blue." Giving a hint costs the team one hint token, so if no hint tokens remain a hint cannot be given. Also, whenever a player gives a hint, the recipient must have at least one card of the chosen rank or suit, e.g., "You have no yellow cards in your hand" is not a legal hint.

There are three ways in which the game may end. If the team makes a third error, the game ends with a score of 0. If the team successfully plays 25 cards, the game ends with perfect score of 25 points. Otherwise, once the deck becomes empty, each player makes one final turn and the game ends with a score equal to the number of fireworks successfully launched.

Hat guessing

We now discuss a strategy for the hat guessing game described in the introduction. We will then generalize this strategy for two colors to an eight color version. The strategy for the eight color hat guessing game will be implemented in both of our strategies for *Hanabi*.

Two color hat guessing game Each of five players will be assigned either a red hat or blue hat at random. Each player will be able to see the color of every other player's hat but will be unable to see the color of her own hat. In some order, for instance from youngest to oldest, each player will then be asked to guess the color of the hat on her own head. The players will be able to hear the guesses made by the previous players, but no other communication is allowed. The objective of the game is for the players to devise a strategy before the hats are assigned that maximizes the expected number of correct guesses they will make as a team.

Since the youngest player has no information about her own hat and has not heard any of the other players' guesses, she can only guess her hat correctly, on average, half of the time. It follows that the expected value of the game can be no greater than 4.5/5 correct guesses.

There is, perhaps surprisingly, a strategy in which the expected number of correct guesses is $4.5/5$. Indeed, suppose that the first player guesses ‘blue’ if the number of blue hats on the heads of the other four players is odd and guesses ‘red’ otherwise. As noted before, this first guess will be correct, on average, half of the time. Once this first guess has been made, every other player can now deduce the color of her own hat! For example, suppose that the second player observes exactly one blue hat on the heads of players three, four, and five. She can now reason that if her hat were blue, the first player would have responded ‘red’ since that indicates there are two blue hats on players two, three, four, and five. By similar reasoning, if her hat were red, the first player would have guessed ‘blue.’ Similarly, players three, four, and five can also deduce the color of the hat they are wearing based upon the first player’s guess.

We now describe a generalized version of this strategy for five players and eight hat colors which we will incorporate into our strategies for *Hanabi*.

Multiple color hat guessing game The following notation will aid in our description of this eight color version of the above hat guessing game. Label the players P_1, P_2, \dots, P_5 and suppose that there are eight different “colors”: $0, 1, \dots, 7$. Let c_i be the color of the hat placed on the head of player P_i . The following generalization of the previous strategy can guarantee at least four of the players will guess correctly.

Player P_1 will guess, or rather respond, with color

$$r_1 := \sum_{i \neq 1} c_i \pmod{8},$$

which is computed by finding the sum of the hat colors of every player who is not the first player and then determining the remainder when divided by 8. Hence, player P_1 is not actually guessing at her own hat color, nor is she guaranteed to respond correctly. However, her response will guarantee that all other players can respond correctly.

For $i > 1$, player P_i will respond

$$r_i := r_1 - \sum_{j \neq 1, i} c_j \pmod{8},$$

where the sum $\sum_{j \neq 1, i} c_j$ adds together the colors of the hats worn by all players other than players P_1 and P_i . Since

$$r_i \equiv \sum_{j \neq 1} c_j - \sum_{j \neq 1, i} c_j \equiv c_i \pmod{8},$$

every player other than the first player is guaranteed to have responded correctly. We remark that this strategy generalizes to any number of colors and any number of players.

We also note that this type of scheme is similar to “check digits” on bar codes such as UPC and ISBN where the final digit of the code serves to verify the parity of the other digits (see, for example, [12]). In the above hat guessing game, each player is missing a different piece of information, and the initial response serves as a “check digit” which allows the other players to deduce the information they are missing.

For more information about this sequential hat guessing game, in addition to other variations, see [3, 4, 8, 11]. While sequential hat guessing games are well understood, many interesting and open problems remain when players guess the colors of their hats simultaneously. See [5, 7, 11] for more information on simultaneous hat guessing.

Overview of applying hat guessing to *Hanabi* The main idea of applying hat guessing to *Hanabi* is that each player’s hand is a “hat” and the contents correspond to a

“color.” While there are more than eight possible hands, we assign each possible hand a “color” 0 through 7. As a result, when a player gives a hint, all other players can determine the colors of their hands, thereby deducing information about its contents.

The two strategies presented assign colors to hands differently. In the first, the color represents which card should be played or discarded. That is, loosely speaking, the colors recommend a particular move to each other player. For the second, more complicated strategy, the colors correspond to a set of possible rank and suit values for a particular card. Hence, each hint narrows down the possibilities for the identity of a particular card.

Strategy 1: The recommendation strategy

In the recommendation strategy, players recommend actions to each other by encoding the recommendations as hints. For example, if player P_1 gives a hint to player P_2 telling her which of her cards are red, *all* of the other players will interpret this as a custom recommended action. For instance, a player may decode this hint to determine that she should discard a certain card in her hand while another player will learn that one of her cards should be played. By implementing a hat guessing scheme, a single hint communicates custom recommendations to each of the other players.

For this strategy, the cards in each player’s hand are indexed from left to right (as seen by the other players), C_1, C_2, C_3, C_4 . Each time a player plays or discards a card, the indices of cards with higher index will shift their indices down by 1, and the new card drawn will be indexed as C_4 .

The key to the recommendation strategy is the following encoding scheme which assigns a number 0 through 7 to each player’s hand. The possible recommendations and their corresponding numbers are as follows:

- | | |
|--------------------|-----------------------|
| 0. Play card C_1 | 4. Discard card C_1 |
| 1. Play card C_2 | 5. Discard card C_2 |
| 2. Play card C_3 | 6. Discard card C_3 |
| 3. Play card C_4 | 7. Discard card C_4 |

Giving recommendations Before we describe how to determine which recommendation to give to each player, we define three types of cards:

- **Playable:** a card that can be successfully played with the current game state.
- **Dead:** a card that has the same rank and suit of a successfully played card.
- **Indispensable:** a card for which all other identical copies have been removed from the game, i.e., a card that if removed from the game will imply a perfect score cannot be obtained.

In Figure 2, player P_2 ’s card C_1 , the white 2, can be successfully played which deems player P_2 ’s card C_1 as *playable*. Player P_4 ’s card C_1 , the green 1, has already been successfully played so player P_4 ’s card C_1 is a *dead card*. Player P_5 ’s card C_4 , the red 5, is *indispensable* since 5’s of each color are unique in the deck. The cards which are playable, dead, and indispensable in a player’s hand will determine the recommendation given to her as described below.

The recommendation for a hand will be determined with the following priority:

1. Recommend that the playable card of rank 5 with lowest index be played.

2. Recommend that the playable card with lowest rank be played. If there is a tie for lowest rank, recommend the one with lowest index.
3. Recommend that the dead card with lowest index be discarded.
4. Recommend that the card with highest rank that is not indispensable be discarded. If there is a tie, recommend the one with lowest index.
5. Recommend that C_1 be discarded.

With this, each player's hand is assigned a number 0 through 7. Viewing the value of the recommendation for each player's hand as the "color of her hat," we see that the player giving a hint would like to tell every other player the color of her hat. Since every other player knows the color of every other player's hat, we can think of this as a multiple color hat guessing game. As discussed in the hat guessing section, if the player giving the hint can communicate a number 0 through 7 to the other players, she can simultaneously tell every other player the color of her hat and thus their custom recommendation. This is possible using the following encoding scheme.

Let position j denote the j th position in the clockwise direction from the player giving the hint.

- | | |
|--|--|
| 0. Rank hint to the player in position 1 | 4. Suit hint to the player in position 1 |
| 1. Rank hint to the player in position 2 | 5. Suit hint to the player in position 2 |
| 2. Rank hint to the player in position 3 | 6. Suit hint to the player in position 3 |
| 3. Rank hint to the player in position 4 | 7. Suit hint to the player in position 4 |

By choosing an appropriate rank or suit, it is indeed always possible to give any of these hints.

Thus when a player gives a hint, she tells every other player the current recommendation for their hands. For example, in Figure 2, player P_1 needs to communicate that the sum of the "colors" of the other players' "hats." She looks at the other players' hands which have values 2, 0, 4, and 0. Since the sum is congruent to 6 modulo 8, she will give a suit hint to player P_4 . From this hint, every other player can determine the color of her hat and know what action has been recommended. For example, player P_2 can deduce the value of her hand is $2 \equiv 6 - (0 + 4 + 0) \pmod{8}$.

It is important to keep in mind that as actions take place after a hint is given, the recommendation made to a player may no longer be appropriate. Consider the situation shown in Figure 3; on her turn, player P_4 will recommend to *both* players P_5 and P_2 to play their blue 3 cards. After which, player P_5 will then play her blue 3 card. In a following turn, player P_2 will also play her blue 3, resulting in an error. Although the player giving the hint could have realized that this conflict was going to occur, our method only allows her to communicate the current state of each hand since this is the only information known to all players. As it is more important for players to communicate in a consistent reliable manner, we must accept these duplicate recommendations as a possibility.

To use the recommendations given to them in a way which reduces the number of errors that will be made, the following algorithm is used:

Action algorithm The action a player will take will be decided in the following order of priority.

1. If the most recent recommendation was to play a card and no card has been played since the last hint, play the recommended card.

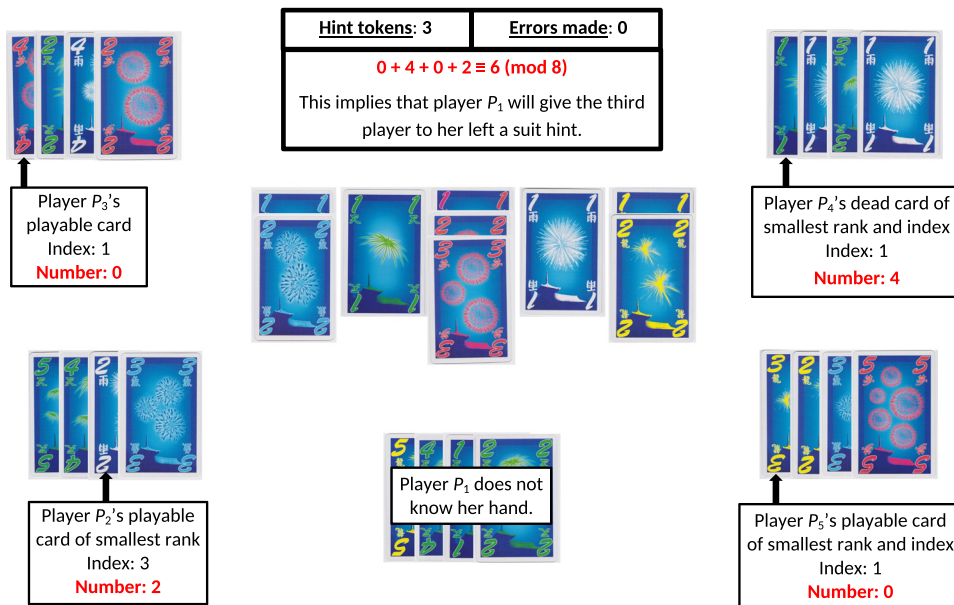


Figure 2 Recommendation strategy: An example of a hint using the recommendation strategy. The updated game state based on this hint and the action algorithm can be found in Figure 3.

2. If the most recent recommendation was to play a card, one card has been played since the hint was given, and the players have made fewer than two errors, play the recommended card.
3. If the players have a hint token, give a hint.
4. If the most recent recommendation was to discard a card, discard the requested card.
5. Discard card C_1 .

To see how the hints and action algorithm fit together, consider Figure 2. Player P_1 gives a suit hint to player P_4 . Recall that player P_2 can decode the hint as $6 - 0 - 4 - 0 \equiv 2 \pmod{8}$. As a result, she knows it is recommended to play her card C_3 .

Similarly, players P_3 and P_5 decode the hint as 0 and are recommended to play C_1 , and player P_4 decodes the hint as 4 receiving the recommendation to discard C_1 . The action algorithm indicates that the next move is for player P_2 to play her card C_3 , which is successful. Since the team has less than two errors, the action algorithm indicates that player P_3 will play her card C_1 , which is also successful. Now, P_4 was recommended to discard C_1 , however, the team has three hint tokens left so the action algorithm tells player P_4 to give a hint. This new hint will give each of the players P_1 , P_2 , P_3 , and P_5 a new recommended action. The updated game state can be seen in Figure 3.

In summary, the recommendation strategy uses hints to tell other players what actions to take. We believe players can implement this strategy with just a little practice, so give it a try at your next game night! Its performance is discussed in the simulation section.

Strategy 2: The information strategy

In the information strategy, hints give players information about the ranks and suits of their cards. Players then decide how to play based upon this knowledge. Once again,

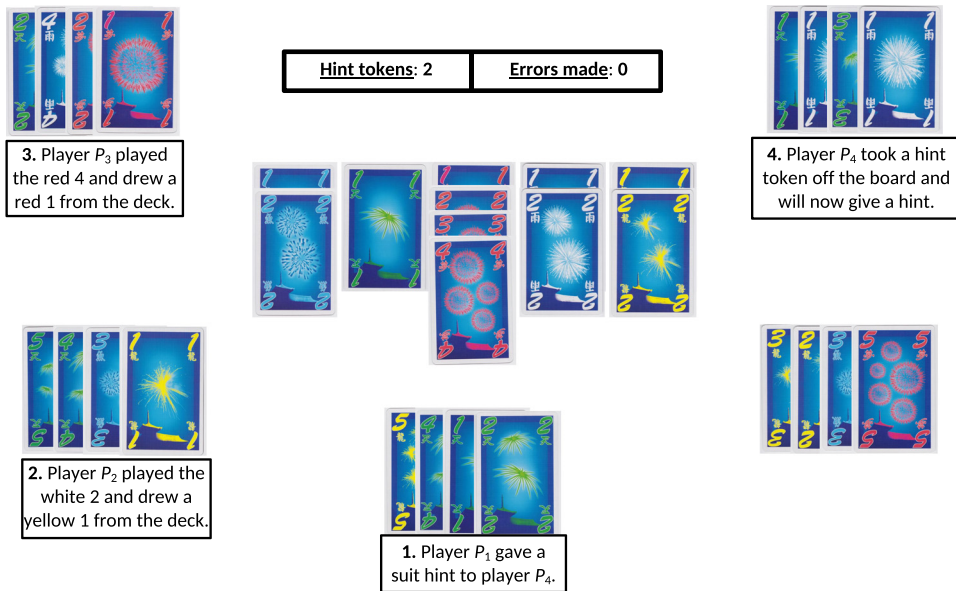


Figure 3 Recommendation strategy: Updated game state three turns after player P_1 gave a hint in Figure 2. It is the beginning of player P_4 's turn after players P_2 and P_3 played the cards based on the recommendations of player P_1 's hint.

a hat guessing scheme will be used so that the player giving the hint can communicate information to all the other players simultaneously. In what follows, we give a brief description of the concepts used in the strategy. The precise implementation of the strategy can be read in the simulation code available online [6].

As with the recommendation strategy, each player's hand will be assigned a value 0 through 7 and the same encoding scheme will be used as in the recommendation strategy. However, unlike the recommendation strategy, the value assigned to the hand of player P_i will not only be a function of the cards in P_i 's hand and the cards played previously, but will also be based upon what P_i has already been able to deduce about the cards in her hand. An important aspect to this deduction will be what we refer to as *public* and *private information*.

Public and private information We refer to two types of information: public and private. Public information is information that all players know; that is, every player knows the same public information. Private information is information that a player can deduce based upon seeing the other players' hands.

For example, in Figure 3, player P_1 has a yellow 5. All of the other players know that they do not have a yellow 5, since there is a unique yellow 5 in the game. However, player P_1 does not know that the other players can deduce that they do not have a yellow 5. Hence, the other players' knowledge that they do not have a yellow 5 is private information. On the other hand, if a hint is given to player P_1 that allows her to deduce that she has a yellow 5, then this knowledge becomes public information.

Another important part of the information strategy is what we call the possibility table, which is based solely on public information.

Possibility table Consider a card in *Hanabi* whose rank and suit are unknown. If no information can be deduced, this card may take on one of five possible ranks and five possible suits. We visualize these possibilities as a 5×5 table that we call the

possibility table. As public information is revealed or deduced about the card, some of these possibilities are eliminated. The table evolves with new information by placing an N in each entry corresponding to a rank and suit combination that is no longer possible and a P in each entry corresponding to rank and suit combination that is possible. Figure 4 depicts what two possibility tables might look like at a certain point in the game.

	1	2	3	4	5
Blue	N	P	P	P	N
Green	N	N	N	N	N
Red	N	N	N	N	N
White	N	N	N	N	N
Yellow	N	N	N	N	N

(a) Possibility table for C_2 .

	1	2	3	4	5
Blue	N	P	P	P	N
Green	P	P	P	P	P
Red	P	P	N	P	P
White	P	N	P	P	P
Yellow	N	N	N	N	N

(b) Possibility table for C_3 .

Figure 4 Possibility tables

Targeting a card When a player gives a hint, that hint will consider exactly one card in every other player's hand. We say the hint *targets* those cards. However, the exact card targeted by each hint may vary from hint to hint. Hence, it is important for all players to know which card is targeted for each hand.

To achieve this, we estimate the probability that each card is playable based upon the public information. To this end, suppose that the card C_i can take on t_i total different values; that is, there are t_i P's in the possibility table for C_i , and a_i of the possibilities for C_i are immediately playable. The probability that card C_i is playable can be estimated by a_i/t_i . However, since there are not the same number of cards of each type in the deck, we use a slightly more complicated scheme to better estimate the probability that the card is playable.

Our more complicated scheme utilizes the publicly available knowledge in the following way. For a card C_i specified by suit and rank, let T_i be the set of elements in the possibility table for C_i with entry 'P' and let S_i be the set of elements in T_i that correspond to playable cards. Now for $c \in T_i$, let m_C be the number of copies of C that have not been fully determined based on publicly available knowledge. The probability that C_i is immediately playable can be estimated by

$$\frac{\sum_{C \in T_i \cap S_i} m_C}{\sum_{C \in T_i} m_C}.$$

The card within a player's hand with the highest such probability is targeted, with the exception that a card with only one P in the possibility table will never be targeted. In the event of a tie, the lowest indexed card is targeted. We remark that in Figure 7 we use the estimate of a_i/t_i for simplicity.

Partition of the possibilities When a player gives a hint, each other player will receive information about her targeted card thereby eliminating some of the P's in the card's possibility table. To establish the meaning of each hint, the set of possibilities for each targeted card is partitioned into 8 sets, and this partition is determined by the public information.

Consider the possibility table for C_3 in Figure 4. There are 16 possible values for C_3 and each hint is one of eight different values, the numbers 0 through 7. As an example,

the players might agree that if the hint is 0, this means that the true value of C_3 is one of the first two possible values in this table, ordered from the top left; that is, either a blue 2 or a blue 3. Similarly, if the hint is a 1, this means that the true value of the card is either a blue 4 or a green 1, and so on. Then when this player receives a hint about C_3 , she is able to eliminate all but two possibilities from the possibility table for C_3 . For example, if the player receives hint 7, then she knows that the true value of C_3 is one of the two last P's in the possibility table. See Figure 5 for an illustration of this.

Note that there many ways to partition the possibility table. While it may seem advantageous to partition it as evenly as above, we will, in fact, partition it differently as we discuss later.

	1	2	3	4	5
Blue		0	0	1	
Green	1	2	2	3	3
Red	4	4		5	5
White	6		6	7	7
Yellow					

	1	2	3	4	5
Blue	N	N	N	N	N
Green	N	N	N	N	N
Red	N	N	N	N	N
White	N	N	N	P	P
Yellow	N	N	N	N	N

(a) The meaning of each hint value for C_3 . (b) Possibility table after receiving the hint 7.

Figure 5 Partition of the possibility table into hint sets for the nearly equal case. Our information strategy uses a slightly different partition shown in Figure 6.

The different hint values partition the possibilities for a card. In the above example, we partitioned the 16 possibilities into eight sets of size two. We will refer to the sets in this partition as *hint sets*. Given any possibility table, there are many different partitions into hint sets. In the C_3 example, as seen in Figure 5, we gave one possible partition for the possibility table of C_3 . Our choice of partition scheme for the information strategy is a little more complex but follows three principles:

1. All possibilities that correspond to dead cards are grouped together in a single hint set. This is because if the card is dead its rank and suit are unimportant.
2. We want many hint sets to contain a single element, which we call *singleton hint sets*. The virtue of this is that whenever a hint specifies a hint set with a single element, the hint recipient learns the exact rank and suit of that card in a single hint. Consequently, we make as many singleton hint sets as possible.
3. Two hints about the same card should always completely determine both the suit and rank of that card. This is accomplished by ensuring that there are no more than eight elements in any hint set. Then after a single hint has been received about a card, there must be fewer than eight possibilities left, at which point a second hint will completely determine the card. We exclude the hint set comprised of the dead cards, which is allowed to have more than eight elements.

As an example, consider again C_3 whose possibility table is given in Figure 4b, and assume that the only dead cards are the 1's of each suit. Then the first hint set consists of the green, red, and white 1's. This leaves 13 possibilities. We can make six singleton hint sets, leaving the seven remaining possibilities for our final hint set. This partition is illustrated in Figure 6.

Value of a hand The *value* of a player's hand, i.e., the hint 0 through 7 that she will be given, is the number assigned to the targeted card by the partition of the possibility table. Note that the possibility table was constructed from public information, so each

	1	2	3	4	5
Blue		1	4	7	
Green	0	2	5	7	7
Red	0	3		7	7
White	0		6	7	7
Yellow					

Figure 6 Partition of the possibility table into hint sets according to the information strategy.

player can determine the value of every other player's hand. Moreover, every player can determine which card in their hand will be targeted and can construct the possibility table for this card. From this information, each player can deduce the partition their card falls into based upon the hint given.

Action algorithm A player will act using her private information with the following priority:

1. Play the playable card with lowest index.
2. If there are less than 5 cards in the discard pile, discard the dead card with lowest index.
3. If there are hint tokens available, give a hint.
4. Discard the dead card with lowest index.
5. If a card in the player's hand is the same as another card in any player's hand, i.e., it is a duplicate, discard that card.
6. Discard the dispensable card with lowest index.
7. Discard card C_1 .

Figure 7 illustrates an example of a player giving a hint using the information strategy with the probability estimate of a_i/t_i . The information strategy is not easily implemented in practice, however a computer implementation is discussed in the following section.

Simulations and their interpretation In this section, the results of simulating the recommendation and information strategies are presented. We also simulate a *cheating strategy* for the purpose of comparison. In this cheating strategy, each player cheats by looking at the cards in their hand and follows the action algorithm presented in the information strategy. The results are presented in Figure 8. The recommendation strategy averages 23.00 points out of 25 and the information strategy averages 24.68 points. By comparison, the perfect information cheating strategy averages 24.87.

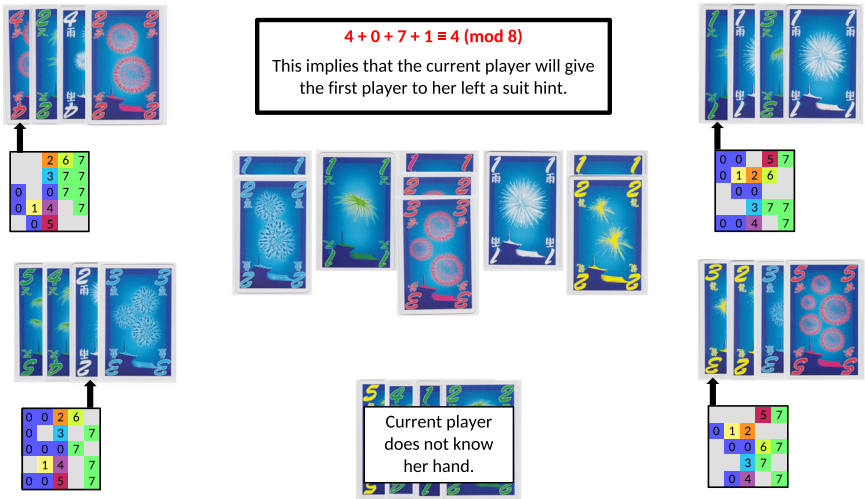
We also remark that in simulation the recommendation strategy frequently makes two errors, but will never make a third. The information strategy will never make any errors.

The simulations were written in C++, and the documented code is available online [6]. The code was designed to be modular, separating the game mechanics from the implementation of player strategies. We would like to encourage any interested readers to improve our strategies or implement their own. We made an effort to make our code accessible and be a versatile foundation upon which any strategy could be implemented.

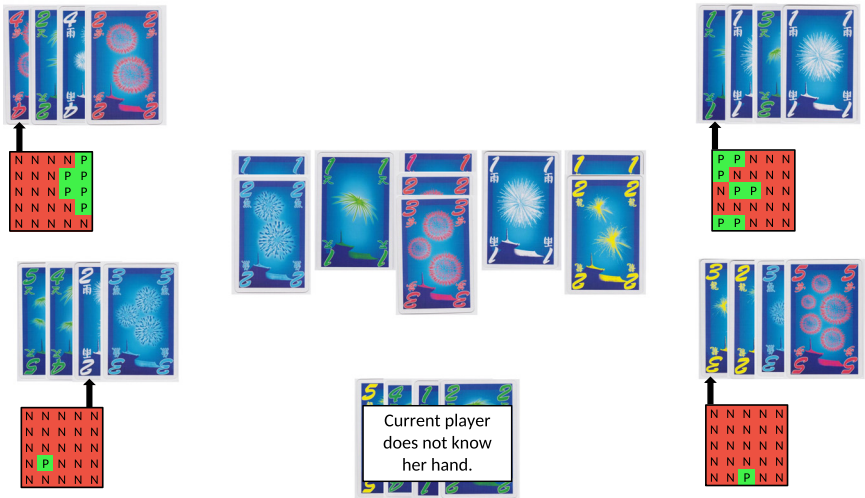
We recognize that our strategies are not optimal. In particular, we see some improvements that could be made but they come at the expense of increased complexity and



(a) The possibility tables and ratio of playable to possible cards for each targeted card.



(b) The corresponding partitions for each targeted card.



(c) Updated possibility tables for each targeted card.

Figure 7 An example of a hint using the information strategy.

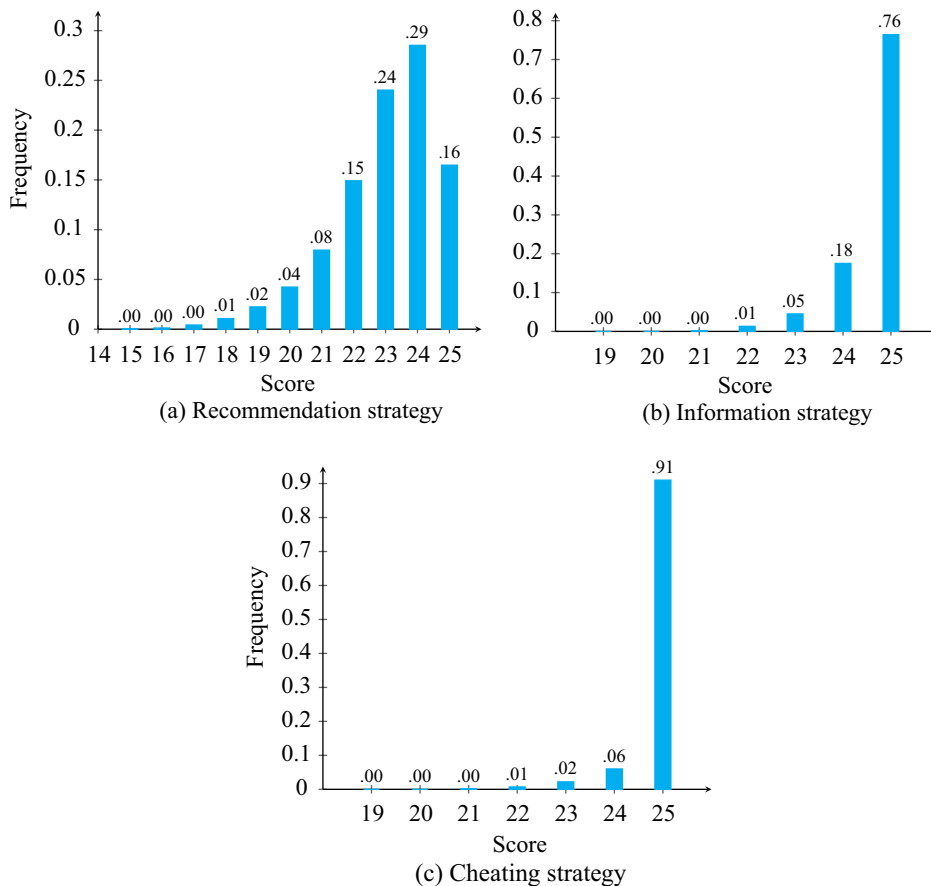


Figure 8 Histograms of the scores after simulating each strategy 10^6 times.

appear to offer only small gains. Although any improvement would be of interest, we would be particularly interested in a strategy that performs significantly better or a simpler strategy with similar performance. We find it important to mention that no strategy can achieve a perfect score every time, as there are permutations of the deck for which a perfect score is impossible. One such permutation occurs when all fifteen 1's are on the bottom of the deck. Thus, there is some upper bound on the average score, which is less than 25. It would be interesting to know a good estimate on the expected value of the game. In particular, we wonder if it is possible for a legal strategy to outperform the average score of 24.87 achieved by our cheating strategy.

Although some of our techniques generalize to other variants, including fewer players, many do not. As such, we leave it to the readers to come up with other strategies for *Hanabi* when playing with fewer than five players. In general, there is still much that could be done regarding the mathematics of *Hanabi*. We hope that fans of *Hanabi* try to implement our strategies and come up with some of their own. Now go out and create your own perfect fireworks display!

Acknowledgment This work was done as part of the inaugural *Rocky Mountain–Great Plains Graduate Research Workshop in Combinatorics* at the University of Denver and the University of Colorado Denver in August 2014. This workshop was additionally co-sponsored by Iowa State University, the University of Nebraska-Lincoln, and the University of Wyoming. Grants supporting this research include National Science Foundation grants CMMI-1300477, CMMI-1404864, DGE-1041000, DMS-1102086, DMS-1301698, and DMS-1427526. We would also like to thank the referees and the editor for their helpful comments.

REFERENCES

1. R. A. Bailey, P. J. Cameron, R. Connelly, Sudoku, gerechte designs, resolutions, affine space, spreads, reguli, and Hamming codes, *Amer. Math. Monthly* **115** no. 5 (2008) 383–404.
2. Board Game Geek, How good is your score really? The statistics (2013), <http://boardgamegeek.com/thread/1005947/how-good-your-score-really-statistics>.
3. E. Brown, J. Tantan, A dozen hat problems, *Math Horizons* **16** no. 4 (2009) 22–25.
4. J. Bushi, *Optimal Strategies for Hat Games*, Master Thesis, Portland State University, Portland, OR, 2012.
5. S. Butler, M. T. Hajiaghayi, R. D. Kleinberg, T. Leighton, Hat guessing games, *SIAM Rev.* **51** no. 2 (2009) 399–413.
6. C. Cox, J. de Silva, P. DeOrsey, F. Kenter, T. Retter, J. R. Tobin, Hanabi Simulation (2015), <https://github.com/rjtobin/HanSim>.
7. U. Feige, *You can leave your hat on (if you guess its color)*. Technical Report MCS04-03, Computer Science and Applied Mathematics, The Weizmann Institute of Science, 2004.
8. J. Havil, *Impossible?: Surprising Solutions to Counterintuitive Conundrums*. Princeton Univ. Press, Princeton, NJ, 2011, 50–59.
9. S. Robinson, Why mathematicians now care about their hat color, *New York Times*, April 2001.
10. S. des Jahres, Spiel des Jahres 2013: Hanabi (2013), <http://www.spiel-des-jahres.com/>.
11. P. Winkler, Games people don't play, *Puzzlers Tribute: A Feast for the Mind* (2002) 301–313.
12. J. Kirtland, *Identification Numbers and Check Digit Schemes*. Mathematical Association of America, Washington, DC, 2001.

Summary. The game of *Hanabi* is a multiplayer cooperative card game that has many similarities to a mathematical “hat guessing game.” In *Hanabi*, a player does not see the cards in her own hand and must rely on the actions of the other players to determine information about her cards. This article presents two strategies for *Hanabi*. These strategies use different encoding schemes, based on ideas from network coding, to efficiently relay information. The first strategy allows players to effectively recommend moves for other players, and the second strategy allows players to determine the contents of their hands. Results from computer simulations demonstrate that both strategies perform well. In particular, the second strategy achieves a perfect score more than 75 percent of the time.

CHRISTOPHER COX (MR Author ID: [1124471](#)) is currently a graduate student at Carnegie Mellon University and enjoys working on problems in extremal and probabilistic combinatorics. If he is not busy being confused by math, then he is probably not working hard enough!

JESSICA DE SILVA (MR Author ID: [1030014](#)) is a graduate student at the University of Nebraska-Lincoln under the supervision of Jamie Radcliffe. If she is not teaching College Algebra at 8AM, she is working out at the university's recreation center. The calories she burns off at the gym are replenished on the weekends when she tries out new restaurants around Lincoln.

PHILIP DEORSEY (MR Author ID: [1124472](#)) received his Ph.D. from the University of Colorado Denver in May 2015 under the direction of William Cherowitzo. He is a new faculty member at Emory & Henry college in Emory, VA. When he is not busy doing math you can usually find him playing games, or hiking on the beautiful trails in southwestern Virginia.

FRANKLIN H. J. KENTER (MR Author ID: [1058998](#)) received his Ph.D. from UC San Diego in 2013 under the supervision of Fan Chung and is currently a Pfeiffer Postdoctoral Instructor in the Computational and Applied Mathematics Department at Rice University. When he is not thinking about spectral graph theory, he is busy devising crazy strategies for games of all sorts.

TROY RETTER (MR Author ID: [1081998](#)) will complete his Ph.D. in spring 2015 under the supervision of Vojtech Rödl at Emory University. Troy is interested in an eclectic mix of discrete mathematics, especially the insights offered by probabilistic combinatorics.

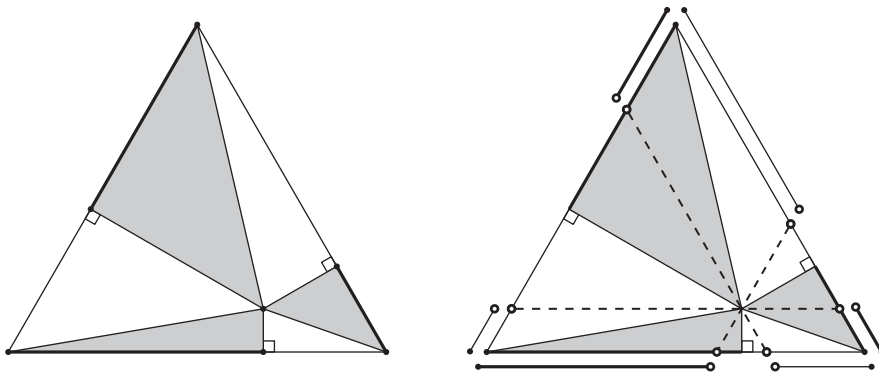
JOSH TOBIN (MR Author ID: [1124473](#)) is a graduate student at UC San Diego, and will be Franklin Kenter's academic brother after graduation. When he is not working on his thesis, he is trying to make his computer write his thesis for him.

Proof Without Words: Half Issues in the Equilateral Triangle and Fair Pizza Sharing

GRÉGOIRE NICOLLIER

University of Applied Sciences of Western Switzerland
1950 Sion, Switzerland
gregoire.nicollier@hevs.ch

An equilateral triangular pizza is divided by six straight cuts going from an arbitrary pizza point to the vertices and to the sides at right angles; two persons share the pizza and the crust fairly by taking alternate slices.



This theorem is certainly old, but we know of no historical source! Various pizza-free proofs with words can be found in [2] (for the crust only) and [3, pp. 153–158]. The fair allocation of a disk—eight equiangular slices from any point of the disk—has a famous proof without words [1]. The dashed subdivision is a fair sharing (except for the crust) exactly when the slices meet on the incircle.

Acknowledgments The author is very grateful to the referee and Gerry Leversha.

REFERENCES

1. L. Carter, S. Wagon, Proof without words: Fair allocation of a pizza, *Math. Mag.* **67** (1994) 267.
2. M. de Villiers, An illustration of the explanatory and discovery functions of proof, *Pythagoras* **33** (2012) Art. #193. <http://dx.doi.org/10.4102/pythagoras.v33i3.193>.
3. *Year Book 2013–2014*. UK Mathematics Trust, University of Leeds.

GRÉGOIRE NICOLLIER (MR Author ID: [989132](#)) is a mountain guide and teaches mathematics in French and in German to engineering students at the University of Applied Sciences of Western Switzerland in Sion (Valais). He studied mathematics at ETH (Ph.D. in homological algebra in 1984). His research interests are focused on polygons, in particular on discrete dynamical systems related to triangles.

How to Divide Things Fairly

STEVEN J. BRAMS

Department of Politics
New York University
New York, NY 10012
USA

steven.brams@nyu.edu

D. MARC KILGOUR

Department of Mathematics
Wilfrid Laurier University
Waterloo, Ontario N2L 3C5
CANADA

mkilgour@wlu.ca

CHRISTIAN KLAMLER

Institute of Public Economics
University of Graz
A-8010 Graz
AUSTRIA

christian.klamler@uni-graz.at

Dividing a set of indivisible items, such as the marital property in a divorce, between two people can be a tricky business when the husband and wife rank the disputed property the same or similarly. But problems can arise even when they rank each item differently, as in this example:

Husband : Sports Car > SUV > Boat > Desk > Couch > Painting

Wife : SUV > Boat > Sports Car > Couch > Painting > Desk

At the outset, things look easy. Because we can give both spouses their first choices, it seems evident we should do exactly that, awarding the sports car to the husband and the SUV to the wife. It also seems clear that we should avoid giving them their last choices, which we can accomplish by awarding the painting to the wife and the desk to the husband.

But that leaves the boat and the couch, and we now have a problem: Both spouses prefer the boat to the couch, so who should get the boat? (Both also prefer the couch to the painting, but precluding the spouses' worst choices took care of this problem: The painting went to the wife, so the couch could go to the husband.)

An alternative approach to dividing marital property would be for the husband and wife to apply an algorithm, such as *alternation*, whereby the spouses take turns, each choosing one item when it is his or her turn. If the spouses are *sincere*—choose in the order of their rankings—and the husband starts, he gets {sports car, boat, desk}, and the wife gets {SUV, couch, painting}. If the wife starts, she does better, obtaining {SUV, boat, couch}, and the husband does worse, obtaining {sports car, desk, painting}. In the latter case, the husband does particularly badly, getting stuck with his worst item (the painting).

The items to be allocated need not be physical goods. For example, they could be committee assignments or project tasks, in which it is stipulated that each person is required to have three. Or they could be chores (“bads” instead of goods), in which case we could ask each person to rank them from least to most burdensome.

Can we go beyond the ad hoc criteria that we began with, such as giving the *players*—who need not be people but could be larger entities, such as organizations or nation-states—their best items and not their worst? This may not always be possible. If we use an algorithm, is there one that avoids the first-chooser bias of alternation, and is it applicable to more than two players?

Properties of Fair Division

The fair division of items, especially if they are indivisible or cannot be shared, is an age-old problem. In this article we describe a simple sequential algorithm, called SA, which seems to have been overlooked in earlier studies [2, 3], for carrying out this division when the players strictly rank items from best to worst. It is less demanding in the information it elicits than are algorithms that ask players to indicate their utilities for items [10], to rank bundles of items [11], or to apply the classic procedure of “divide-and-choose” [9, 10].

We begin by specifying the properties of an allocation for two or more players that it would be desirable to satisfy. Although SA uses only players’ rankings, one of the four properties we describe below uses the *Borda score* of an item as one measure of its utility to a player: A lowest-ranked item receives 0 points, the next-lowest 1 point, and so on. A player’s Borda score is the sum of its points for the subset of items it receives, which may be thought of as one possible cardinalization (into utilities) of the ranks. In the absence of the players’ actual utilities for the items, which we assume to be additive, it is the only one we use in the subsequent analysis.

The properties of allocations that we analyze are the following, whose two-letter abbreviations we also use as adjectives in describing allocations:

- *Efficiency or Pareto-Optimality (PO)*: There is no other allocation that is at least as preferred by all players and strictly preferred by at least one.
- *Envy-freeness (EF)*: Each player values the set of items it receives at least as much as the set of items received by any other player.
- *Maximality (MX)*: The allocation maximizes the minimum rank of the items received by any player.
- *Borda Maximality (BMX)*: The allocation maximizes the minimum Borda score of the items received by any player.

MX ensures that the rank of the least-preferred item that any player receives is as high as possible [7, 12], whereas BMX ensures that the Borda score of the player with the lowest score is as high as possible [8]. As we will show, different allocations may satisfy each of these properties.

Because SA requires only that players rank items, we need a definition of envy-freeness that enables players to compare the value of their items with the value of the items received by the other players. We say that a player, say *A*, does not envy another player, say *B*, if and only if there is an injection (a 1-1 mapping) from *A*’s items into *B*’s items such that *A* prefers each of its items to the item of *B* to which it is mapped [8]. An allocation is *item-wise envy-free* (EF) if and only if no player envies any other.

To illustrate this definition in the two-person example we discussed in the introduction, assume that the husband receives {sports car, boat, desk} and the wife receives {SUV, couch, painting}. Then we can map item-wise the husband’s items into the wife’s such that he prefers each of his items to his wife’s:

sports car > SUV; boat > couch; desk > painting.

Although there is a mapping for the wife such that she prefers two of her items to two of her husband's,

$$\text{SUV} > \text{sports car}; \text{painting} > \text{desk},$$

it is not true that $\text{couch} > \text{boat}$ for her. Indeed, no allocation of three items to each spouse makes possible a 1-1 mapping such that each spouse item-wise prefers each of his or her items to the items of the other spouse. Thus, this example does not admit an EF allocation, based on item-wise comparisons.

The Sequential Algorithm (SA) and Examples

SA works in stages. We illustrate it with four examples in this section and also discuss its properties. In the following section we will prove more general results.

We assume that there are $n \geq 2$ players and $m = kn$ distinct items to be allocated, where k is a positive integer. If m is not a multiple of n (e.g., if $n = 2$ and m is odd), the “extra” items might be distributed to the players at random—with a maximum of one to each player—after SA has been applied.

SA produces an *equal* allocation, in which each player receives the same number k of items. If the allocation is not equal, it is not possible to make item-by-item comparisons, which our definition of EF assumes. We recognize that unequal allocations may be envy-free—based on the utilities that players have for their subsets of items, compared with the utilities they attribute to the subsets of items of the other players—but we cannot make this comparison based only on players' ranks.

The allocation rules of SA, which give one item to each player on each round, are the following:

- (i) On the first round, descend the ranks of the players, one rank at a time, stopping at the first rank at which each player can be given a different item (at or above this rank). This is the *stopping point* for that round; the rank reached is its *depth*, which is the same for each player. Assign one item to each player in all possible ways that are at or above this depth (there may be only one), which may give rise to one or more SA allocations.
- (ii) On subsequent rounds, continue the descent, increasing the depth of the stopping point on each round. At each stopping point, assign items not yet allocated in all possible ways until all items are allocated.
- (iii) At the completion of the descent, if SA gives more than one possible allocation, choose one that is efficient (PO) and, if possible, EF.

The process of descent is the same as that of “fallback bargaining” [4], but its purpose is the fair division of items, not reaching an outcome acceptable to some (e.g., a simple majority) or all of the players.

We next give examples that illustrate rules (i)–(iii) when $n = 2$; later we analyze an example in which $n = 3$. The players are A, B, \dots , and the items they rank are $1, 2, \dots$. Players rank items in descending order of preference.

Example 1:

$$A : \underline{1} \ 2 \ \underline{3} \ 4$$

$$B : \underline{2} \ 3 \ \underline{4} \ 1$$

The stopping point of round 1 is depth 1, where A obtains item 1 and B obtains item 2. At depth 2 we cannot give different items to the players, because item 2 has already

been given to B , so in round 2 we must descend to depth 3 to give the players different items (item 3 to A and item 4 to B).

We have underscored the items that each player receives. Because this exhausts the items, we are done, which yields the unique SA allocation of (13, 24) to (A , B). Henceforth, we list the players in alphabetical order, and their items in the order in which the players rank them.

Observe that on each round, each player prefers the item it receives to the item that the other player receives (for A , item 1 > item 2 and item 3 > item 4; for B , item 2 > item 3 and item 4 > item 1). Hence, there is a 1-1 mapping of A 's items into B 's, and B 's items into A 's, such that each player prefers its items to the other player's items. Therefore, the allocation (13, 24) is EF.

This allocation does *not* depend on a player's utilities for items, which we assume are consistent with their rankings (i.e., higher-ranked items have greater utility than lower-ranked items) and additive. Other two-item allocations, such as (12, 34), are not item-wise EF, because there is no 1-1 mapping of B 's items to A 's such that B prefers each of its items to the items to which it is mapped. In particular, notice in B 's ranking that items 2 and 1 bracket items 3 and 4, so B may prefer the combination of items 2 (best) and 1 (worst) to the combination of items 3 and 4 (two middle-ranked items).

For example, if B 's utilities for items 1, 2, 3, and 4 are 1, 5, 3, and 2, then B 's utility for its subset of items, 34, is 5, and its utility for A 's subset of items, 12, is 6, so B will envy A . But if B 's utilities are 1, 6, 5, and 4, then it values its subset at 9 and A 's subset at 7, so in this case B will not envy A . Only allocation (13, 24) is EF for all possible utilities of the players consistent with their rankings.

It is easy to see that (13, 24) is PO, because there is no allocation that is at least as preferred by both players. We say that (13, 24) is *Pareto-superior to*, or *Pareto-dominates*, another allocation—say, the “reverse” allocation, (24, 13)—because $1 > 2$ and $3 > 4$ for A , and $2 > 3$ and $4 > 1$ for B . In Example 1 no allocation is Pareto-superior to (13, 24), which means that (13, 24) is PO.

In general, an allocation is PO if and only if it is the product of a *sequence of sincere choices* by the players [8], whereby each player chooses its best available item on its turn. Thus, if the players choose items in the order $ABAB$, they obtain (13, 24); if they choose in the order $AABB$, they obtain (12, 34), so both these allocations are PO. By comparison, no sincere sequence yields the allocation (24, 31), so it is not PO.

The allocation (13, 24) is also MX; the only other allocation of two items to each player that gives neither player a worst item is (12, 34), rendering it also MX. However, (12, 34) is *not* BMX, because it gives Borda scores of (5, 3) to (A , B), making B 's score less than the score of 4 that each player receives from (13, 24).

If SA gives two or more allocations, only one may be MX. This is true of the two SA allocations—one on the left, the other on the right—in our next example (the vertical lines are explained below):

Example 2:

$$\begin{array}{ll} A : \underline{1} \underline{2} \underline{3} \underline{4} \underline{5} | \underline{6} \underline{7} \underline{8} & A : \underline{1} \underline{2} \underline{3} \underline{4} \underline{5} | \underline{6} \underline{7} \underline{8} \\ B : \underline{3} \underline{4} \underline{5} \underline{6} \underline{7} | \underline{8} \underline{1} \underline{2} & B : \underline{3} \underline{4} \underline{5} \underline{6} \underline{7} | \underline{8} \underline{1} \underline{2} \end{array}$$

In the first two rounds, SA gives (12, 34) to (A , B), reaching depth 2 in both allocations. In round 3, the stopping point is depth 5 for both the left and right allocations, as shown by the vertical lines, but now there is some choice in the items we give to A and B . In particular,

- (i) the left-hand allocation gives items (5, 6) to (A , B) at depth 5, followed in round 4 by items (7, 8) at depth 7, resulting in (1257, 3468);

- (ii) the right-hand allocation gives items (5, 7) to (A, B) at depth 5, followed in round 4 by items (6, 8) at depth 6, resulting in (1256, 3478).

Clearly the right-hand allocation, with a maximum depth of 6, is MX. Note that all allocations must have depth 6 or greater; otherwise, item 8 would not be assigned to either player.

The right-hand allocation (1256, 3478) is also BMX, giving (A, B) Borda scores of (18, 18)—a minimum score of 18—whereas the left-hand allocation (1257, 3468) gives the players scores of (17, 19) for a minimum score of 17. (An exhaustive search shows that no other allocation, even among allocations in which players receive different numbers of items, gives a greater minimum than 18.) Thus, while both allocations are EF and PO, only the right-hand allocation is MX and BMX.

Example 2 illustrates how SA can result in more than one allocation that is PO and EF, but only one is MX or BMX in this example. Our next example illustrates that if both players rank the same item last, there cannot be an EF allocation:

Example 3:

$$\begin{array}{ll} A : \underline{1} \ 2 \ \underline{3} \ \underline{4} \ 5 \ 6 & A : \underline{1} \ 2 \ \underline{3} \ 4 \ 5 \ \underline{6} \\ B : \underline{2} \ 3 \ \underline{5} \ 4 \ 1 \ \underline{6} & B : \underline{2} \ 3 \ \underline{5} \ \underline{4} \ 1 \ 6 \end{array}$$

In rounds 1 and 2, with stopping points at depth 1 and depth 3, the left-hand and right-hand allocations coincide, giving 13 to A and 25 to B . In round 3, the stopping point is depth 6 for both allocations, the lowest possible, but items 4 and 6 are assigned in two different ways.

The player who receives item 6 must be envious, because no 1-1 mapping can map item 6 to a less-preferred item. Thus, the allocation of items in Example 3 is not EF, although the partial allocation of the first four items to both players at depths 1 and 3 is. Both complete allocations are MX (maximum depth of 6) and BMX (minimum Borda score of 8).

Our final example in this section, which duplicates the rankings of the husband (A) and wife (B) in the introduction, illustrates that an SA allocation may fail to be EF even when the players rank every item differently (we illustrated this failure earlier for alternation but not for SA):

Example 4:

$$\begin{array}{ll} A : \underline{1} \ 2 \ 3 \ \underline{4} \ \underline{5} \ 6 & A : \underline{1} \ 2 \ \underline{3} \ 4 \ 5 \ 6 \\ B : \underline{2} \ \underline{3} \ 1 \ 5 \ \underline{6} \ 4 & B : \underline{2} \ 3 \ 1 \ \underline{5} \ \underline{6} \ 4 \end{array}$$

Here the problem arises in round 2, with the stopping point at depth 4, where the left-hand allocation gives 14 to A and 23 to B , whereas the right-hand allocation gives 13 to A and 25 to B . Whoever receives the lower-ranked item in round 2 will be envious, because no 1-1 matching can map every item of that player to a lower-ranked item of the other player. Despite the fact that each player ranks the six items differently, and no player receives a worst item in either SA allocation, neither allocation in Example 4 is EF.

In Example 4, both allocations are MX (in the descent, the depth reaches 5 when the allocations are complete); moreover, they are equal according to BMX, with Borda scores of 10 to the advantaged player and 8 to the disadvantaged player, so the minimum Borda score of each allocation is 8. According to both MX and BMX, therefore, the two allocations in Example 4, unlike Example 3, are equally fair to the players.

When $n = 2$, there is a simple condition, called “Condition D” [6], for determining whether an EF allocation can exist: For every odd i , the two players’ sets of top i items are *not* identical. In Example 3, A ’s and B ’s top 5 items are identical, and in Example 4, their top 3 items are identical, so neither example yields an EF allocation. This is not true for the top 1 and top 3 items in Example 1, nor the top 1, 3, 5, and 7 items in Example 2, so in both of these examples an EF allocation exists which, as we showed, SA finds.

To summarize, SA may give a unique PO-EF allocation (Example 1) or multiple PO-EF allocations (Example 2), only one of which—possibly not the same one—is MX or BMX. In addition, SA may not produce an EF allocation (Examples 3 and 4), even when the players rank all items differently (Example 4), because no EF allocation exists.

Properties of SA

If all items can be allocated in an EF way, we say there is a *complete EF allocation*. For $n = 2$, Brams, Kilgour, and Klamler [6] provide an algorithm, AL (for “algorithm”), which finds at least one complete PO-EF allocation if one exists (though not necessarily all of them, as we will see). Furthermore, when there is no complete EF allocation, as in Examples 3 and 4, AL finds the largest and most preferred subset of items that can be allocated in an EF way. Items that cannot be so allocated (e.g., items 4 and 6 in Example 3; items 3 and 6 in Example 4) are placed in a “contested pile,” to which another algorithm, called undercut, can be applied [1, 5].

By contrast, SA always allocates all items. As illustrated in Examples 3 and 4, SA yields an allocation that may be EF only on some rounds, rendering the allocation only partially EF.

Although SA may not give a complete EF allocation, it always produces at least one PO allocation. Moreover, this is true however many players there are (i.e., for all $n \geq 2$).

Theorem 1. *SA rules (i) and (ii) produce at least one allocation that is PO.*

Proof. Under SA, all items are allocated one at a time to the players and ranked at or above each stopping point in the descent process. Because each allocation gives equal numbers of items to the players, a non-SA allocation must give at least one player an item it ranks below some item that it would receive under SA. This proves that no non-SA allocation can be Pareto-superior to any SA allocation. Because Pareto-superiority is irreflexive and transitive, at least one of the SA allocations—say, X —must be maximal with respect to Pareto-superiority within the set of SA allocations. Because no non-SA allocation can be Pareto-superior to X , X must be PO. ■

Theorem 1 guarantees that at least one PO allocation survives the application of rule (iii). Our next example shows that rule (iii) has bite—not every SA allocation need be PO. This example also shows that not all allocations given by AL, which duplicate those given by SA in Example 5, need be “locally Pareto-optimal,” as we incorrectly claimed in [6].

Example 5:

$$\begin{array}{ll} A : \underline{1} \underline{2} \underline{3} \underline{4} \underline{5} | \underline{6} \underline{7} \underline{8} & A : \underline{1} \underline{2} \underline{3} \underline{4} \underline{5} | \underline{6} \underline{7} \underline{8} \\ B : \underline{7} \underline{8} \underline{1} \underline{2} \underline{3} | \underline{5} \underline{4} \underline{6} & B : \underline{7} \underline{8} \underline{1} \underline{2} \underline{3} | \underline{5} \underline{4} \underline{6} \end{array}$$

At the completion of round 2, SA gives (12, 78) to (A , B), stopping at depth 2. The next stopping point is at depth 5, indicated by the vertical lines, where B must receive

item 3 in round 3. There is, however, a choice for A : The left-hand allocation gives item 4 to A , and the right-hand allocation gives item 5 to A .

Continuing, the left-hand allocation gives items 6 and 5, respectively, to A and B in round 4, with the stopping point at depth 6, whereas the right-hand allocation gives items 6 and 4 to A and B , respectively, in round 4, with the stopping point at depth 7. Because both players prefer the last two items they receive in the left-hand allocation to those that they receive in the right-hand allocation, the left-hand allocation Pareto-dominates the right-hand allocation, so only the left-hand allocation is PO.

Interestingly enough, both SA allocations in Example 5 are complete EF allocations, even though only one is PO, showing that EF does not imply PO. The converse also fails because, for example, an allocation that gives one player only its top items will generally make another player envious. Thus, PO and EF are independent properties.

In Example 5, the left-hand allocation (1246, 7835) is MX (its maximum depth is 6). An exhaustive search of equal and unequal allocations shows that it is also BMX, with Borda scores of (19, 18), compared with Borda scores of (18, 17) for the right-hand allocation.

But SA does not invariably find a PO-EF allocation that—based on the properties of MX or BMX—is superior to a non-SA allocation, as our next example illustrates.

Example 6:

$$\begin{array}{ll} A : \underline{1} \underline{2} \underline{3} \underline{4} 5 6 7 8 & A : \underline{1} \underline{2} \underline{3} \underline{4} \underline{5} 6 7 8 \\ B : \underline{8} \underline{7} \underline{6} 3 2 1 \underline{5} 4 & B : \underline{8} \underline{7} \underline{6} \underline{3} 2 1 5 4 \end{array}$$

The SA allocation is shown on the left. In the first three rounds, at depths 1, 2, and 3, SA allocates (123, 876) to (A , B). On round 4 and at depth 7, A and B receive, respectively, items 4 and 5, producing the allocation (1234, 8765).

But the non-SA allocation (1245, 8763) on the right is of depth 5. Moreover, it is not only MX but also BMX, giving Borda scores of (20, 22), compared with (22, 19) for the SA allocation. Both the left-hand and the right-hand allocations are EF and PO. We will return to this example later to show that there are seven distinct complete EF allocations, but only the aforementioned two are PO.

Both the left-hand (SA) and the right-hand (non-SA) allocations in Example 6 are complete EF and PO (A prefers the former, and B the latter, when each player obtains its four best items). AL gives only the SA allocation, so like SA, it does not always find all PO-EF allocations—including those that might be MX or BMX (e.g., the non-SA allocation on the right in Example 6)—as we incorrectly stated in [6].

Although at least one SA allocation is PO by Theorem 1, it may not be EF, as we showed in Examples 3 and 4. But if there is an EF allocation when $n = 2$, we have the following result.

Theorem 2. *Let $n = 2$. If an EF allocation exists, then SA will give at least one allocation that is EF and PO.*

Proof. We earlier mentioned Condition D (see Example 4)—that an EF allocation exists if and only if, for all odd k , at least one of A 's k most preferred items is not one of B 's k most preferred items. Another necessary and sufficient condition for an allocation to be EF is that the item that each player receives on the j th round is among the player's top $2j - 1$ items [6].

Assume Condition D holds. Taking $k = 1$, it is clear that A 's and B 's most preferred items are different, so on round $j = 1$, SA must allocate to each player its most preferred item, and the stopping depth d_j is $d_1 = 1$.

Now assume that, up to the completion of round j , SA has allocated j of each player's top $2j - 1$ items, and the stopping depth on round j is $d_j \leq 2j - 1$. Consider round $j + 1$. Combined, the preference orderings of A and B account for either 2, 3, or 4 distinct additional items at depth $2j$ or $2j + 1$. Therefore, to assign an additional item to both A and B from their top $2j + 1$ items, it is necessary to increase the stopping depth to at most $d_j + 2$.

If there is a choice, ensure that a player does not prefer any unassigned item to the item it receives. It follows that $d_{j+1} \leq 2j + 1$, and that the $(j + 1)$ st item received by each player is among its $2j + 1$ most preferred items. Therefore, the resulting SA allocation is EF. Moreover, it is PO, because it is the result of a sequence of sincere choices (as discussed after Example 1). ■

When $n = 2$, it is relatively easy to determine whether a given allocation is EF, PO, MX, or BMX. It is considerably more complex to find *all* allocations that are, say, EF.

To illustrate this calculation, recall from Example 6 that we gave a non-SA equal allocation that improved upon the SA allocation in terms of MX and BMX, but we did not prove that it was the only such allocation, or that there was not another allocation that better satisfied one or both of these properties. To analyze Example 6 in detail, we list all possible item-by-item allocations at each odd depth.

Example 6 (repeated):

$A : 1\ 2\ 3\ 4\ 5\ 6\ 7\ 8$

$B : 8\ 7\ 6\ 3\ 2\ 1\ 5\ 4$

At depth 1, (A, B) must receive items $(1, 8)$. Then, at depth 3, (A, B) must receive, in addition, one of $(2, 7)$, $(2, 6)$, $(3, 7)$, or $(3, 6)$. Finally, at depth 5 and again at depth 7, (A, B) must receive pairs of items that depend on the items already received. The details are shown in Table 1, which includes all EF allocations for Example 6, as well as their MX depths and Borda scores, illustrating that the determination of all EF allocations and their properties may be combinatorially complex.

As Table 1 shows, there are seven EF allocations, labeled a, b, c, d, e, f , and g , which we call *classes*, that can be reached in a total of 21 different ways. Specifically, there are 7 a 's, 4 b 's, 2 c 's, 1 d , 1 e , 5 f 's, and 1 g . The MX depths and Borda scores depend only on the class, not on the way it was obtained. These scores are shown only for the first member of each class.

The MX depths of the b 's and the f 's are minimal (i.e., 5), but only the b 's have a maximin Borda score (20). This verifies that allocation b (1245, 8765) is indeed MX and BMX. It and the unique SA allocation (allocation 1 in class a) are the only PO allocations.

So far we have not illustrated SA with examples in which $n > 2$. While its application to the division of items among three or more players is straightforward, if more tedious, SA no longer ensures that if there is a complete EF allocation, it will be chosen by SA when $n > 2$.

Example 7:

$A : \underline{1}\ \underline{2}\ 3\ 4\ 5\ \underline{6}\ 7\ 8\ 9$

$B : \underline{5}\ \underline{8}\ 1\ 2\ 6\ \underline{7}\ 3\ 4\ 9$

$C : \underline{3}\ \underline{4}\ \underline{9}\ 1\ 2\ 5\ 6\ 7\ 8$

SA allocates items $(1, 5, 3)$ to (A, B, C) at depth 1; then $(2, 8, 4)$ at depth 2; and finally $(6, 7, 9)$ at depth 6. Notice that B may envy A for obtaining items $\{1, 2, 6\}$, which fall

TABLE 1: EF Allocations, MX Depths, and Borda Scores for Example 6

Allocation	Depth ≤ 3	Depth ≤ 5	Depth ≤ 7	Complete	MX Depth	BMX Score
1	(2, 7)	(3, 6)	(4, 5)	(1234, 8765)- <i>a</i>	7	(22, 19)
2		(4, 6)	(3, 5)	(1243, 8765)- <i>a</i>		
3			(5, 3)	(1245, 8763)- <i>b</i>	5	(20, 22)
4		(4, 3)	(5, 6)	(1245, 8736)- <i>b</i>		
5			(6, 5)	(1246, 8735)- <i>c</i>	7	(19, 18)
6		(5, 6)	(4, 3)	(1254, 8763)- <i>b</i>		
7		(6, 3)	(4, 5)	(1264, 8735)- <i>c</i>		
8	(2, 6)	(3, 5)	(4, 7)	(1234, 8657)- <i>a</i>		
9		(4, 3)	(5, 7)	(1245, 8637)- <i>b</i>		
10			(7, 5)	(1247, 8635)- <i>d</i>	7	(18, 17)
11	(3, 7)	(2, 6)	(4, 5)	(1324, 8765)- <i>a</i>		
12		(4, 6)	(2, 5)	(1342, 8765)- <i>a</i>		
13		(4, 2)	(6, 5)	(1346, 8725)- <i>e</i>	7	(18, 17)
14			(5, 2)	(1345, 8762)- <i>f</i>	5	(19, 21)
15		(5, 6)	(4, 2)	(1354, 8762)- <i>f</i>		
16		(5, 2)	(4, 6)	(1354, 8726)- <i>f</i>		
17	(3, 6)	(2, 7)	(4, 5)	(1324, 8675)- <i>a</i>		
18		(2, 5)	(4, 7)	(1324, 8657)- <i>a</i>		
19		(4, 2)	(5, 7)	(1345, 8627)- <i>f</i>		
20			(7, 5)	(1347, 8625)- <i>g</i>	7	(17, 16)
21		(5, 7)	(4, 2)	(1354, 8672)- <i>f</i>		

Note: At depth 1, the 21 complete EF allocations give items (1, 8) to (A, B) . At lower depths, they fall into seven classes (7 *a*'s, 4 *b*'s, 2 *c*'s, 1 *d*, 1 *e*, 5 *f*'s, 1 *g*), each of which gives the same complete allocation but different items at different maximum odd depths. The MX depths, and the BMX scores, are shown only for the first member of each class. The MX depths of the *b*'s and the *f*'s are minimal (5), but only the *b*'s have a maximin Borda score (20). The *a*'s and the *b*'s are the only two classes that yield PO allocations, with the first *a* allocation (allocation 1) being the unique SA allocation.

between B 's two best items (items 5 and 8) and its sixth-best item (item 7). Because A 's items bracket B 's, it follows that there is no 1-1 mapping of B 's items to A 's such that B always prefers its own item to the item of A to which it is mapped. Thus, this allocation is not EF.

However, by switching items 6 and 7 between A and B in the SA allocation, we obtain a non-SA allocation, as demonstrated below.

Example 7 (cont.):

$A : \underline{1} \underline{2} 3 4 5 6 \underline{7} 8 9$

$B : \underline{5} \underline{8} 1 2 \underline{6} 7 3 4 9$

$C : \underline{3} \underline{4} \underline{9} 1 2 5 6 7 8$

To show that the allocation (127, 586, 349) is EF, observe that C gets its three best items, so it cannot do better and, therefore, will not be envious. But now it is easy to check that the required 1-1 mappings of A 's items to B 's, B 's to A 's, and A 's and B 's to C 's, all exist, confirming that the allocation is EF.

As illustrated in Example 1, we can similarly demonstrate that the SA allocation in Example 7 is PO with the sequence of sincere choices, $ABCABCCAB$. To demonstrate

that the non-SA allocation is also PO, we can use the sequence of sincere choices, *ABCABCCBA*.

Although not EF, the SA allocation in Example 7 has the advantage of being both MX and BMX. It gives *A* and *B* at worst a sixth-best item, whereas the non-SA allocation gives *A* a seventh-best item. Similarly, the SA allocation gives Borda scores of (18, 18, 21) to (*A*, *B*, *C*), whereas the EF allocation gives the players Borda scores of (17, 19, 21), so the SA allocation gives a higher minimum. Clearly there are trade-offs among our properties, and which should take priority may be open to debate.

As a final property of SA, we consider its vulnerability of manipulation. Not surprisingly, if $n = 2$ and one player (say, *A*) has complete information about the preferences of the other player (*B*), and *B* is sincere, *A* can exploit *B*, as shown in our next example.

Example 8:

$$\begin{aligned} A : & \underline{1} \underline{2} \underline{3} \underline{4} 5 6 \\ B : & \underline{6} \underline{3} \underline{5} \underline{4} 2 1 \end{aligned}$$

The SA allocation is underscored, with *B* receiving its three top items and *A* not doing quite so well. But now assume that *A* insincerely indicates its preferences to be those shown below, with *B*'s preferences remaining the same.

Example 8 (cont.):

$$\begin{aligned} A' : & \underline{3} \underline{1} \underline{2} 4 5 6 \\ B : & \underline{6} \underline{3} \underline{5} \underline{4} 2 1 \end{aligned}$$

This SA allocation shows that *A*'s insincere preferences turn its original disadvantage into an advantage by giving it its three top items, whereas *B* now does worse.

Although not strategy-proof, SA seems relatively invulnerable to strategizing in the absence of any player's having complete information about its opponent's or opponents' preferences. The manipulator's task is further complicated if the other players are aware that an opponent might try to capitalize on its information and, consequently, they take countermeasures (e.g., through deception) to try to prevent their exploitation.

Summary and Conclusions

To summarize, we have shown that if $n \geq 2$, SA always yields at least one PO allocation and, if $n = 2$, SA always yields an allocation that is PO and EF, provided an EF allocation exists. Although, initially, SA may produce some allocations that are not PO, these will be eliminated by invoking SA rule (iii). The set of PO-EF allocations that SA produces, however, may not include one that satisfies the properties of MX or BMX, although our examples suggest that it probably will not be far off.

If $n > 2$, SA may fail to yield an EF allocation when one exists. In such a case, however, an SA allocation may have redeeming properties, such as be MX or BMX. While SA is not strategy-proof even when $n = 2$, in most real-life cases it is unlikely that one player would have sufficient information about another player's preference rankings—not to mention be able to formulate a strategy that would exploit such information—to manipulate it successfully.

SA seems most applicable to allocation problems in which there are numerous small items, which need not be physical goods, as we noted earlier. If there is one big item that two players desire (e.g., the house in a divorce), it may not be possible to prevent

envy, especially because SA specifies that each player must receive the same number of items. (This stipulation may be viewed as essential to achieving fairness in some, but certainly not all, situations.) In such a case, the most practical solution might be to sell the big item—in effect, making it divisible—and divide the proceeds.

Other modifications in SA might include not restricting the allocation of items of one to each player on every round, and relaxing the assumption that the number of items is an integer multiple of the number of players. These modifications would change the fair-division problem fundamentally, however, because properties like EF, MX, and BMX would have to be redefined to take into account that players may not receive the same number of items.

Acknowledgment The authors thank the editor and two referees for valuable suggestions that have substantially improved this article. Klamler was supported by the University of Graz project “Wahl-Auswahl-Entscheidung.”

REFERENCES

1. H. Aziz, A note on the undercut procedure, *Social Choice Welfare* **45** (2015) 723–728.
2. S. Bouveret, Y. Chevaleyre, N. Maudet, Fair allocation of indivisible goods. In *Handbook of Computational Social Choice*. Ed. F. Brandt, V. Conitzer, U. Endriss, J. Lang, A. D. Procaccia. Cambridge Univ. Press, Cambridge, UK, 2016.
3. S. J. Brams, P. H. Edelman, P. C. Fishburn, Fair division of indivisible items, *Theory Decis.* **55** no. 2 (2003) 147–180.
4. S. J. Brams, D. M. Kilgour, Fallback bargaining, *Group Decis. Negotiation* **10** no. 4 (2001) 287–316.
5. S. J. Brams, D. M. Kilgour, C. Klamler, The undercut procedure: An algorithm for the envy-free division of indivisible items, *Social Choice Welfare* **39** nos. 2–3 (2012) 615–631.
6. S. J. Brams, D. M. Kilgour, C. Klamler, Two-person fair division of indivisible items: An efficient, envy-free algorithm, *Not. AMS* **61** no. 2 (2014) 130–141.
7. S. J. Brams, D. M. Kilgour, C. Klamler, Maximin envy-free division of indivisible items (to be published).
8. S. J. Brams, D. L. King, Efficient fair division: Help the worst off or avoid envy?, *Ration. Soc.* **17** no. 4 (2005) 387–421.
9. S. J. Brams, A. D. Taylor, *Fair Division: From Cake-Cutting to Dispute Resolution*. Cambridge Univ. Press, Cambridge, UK, 1996.
10. S. J. Brams, A. D. Taylor, *The Win-Win Solution: Guaranteeing Fair Shares to Everybody*. W. W. Norton, New York, 1999.
11. D. Herreiner, C. Puppe, A simple procedure for finding equitable allocations of indivisible goods, *Social Choice Welfare* **19** no. 2 (2002) 415–430.
12. A. D. Procaccia, J. Wang, Fair enough: Guaranteeing approximate maximin shares. *Proceedings of the 14th ACM Conference on Economics and Computation* (2014) 675–692.

Summary. We propose an intuitively simple sequential algorithm (SA) for the fair division of indivisible items that are strictly ranked by two or more players. We analyze several properties of the allocations that it yields and discuss SA’s application to real-life problems, such as dividing the marital property in a divorce or assigning people to committees or projects.

STEVEN J. BRAMS (MR Author ID: [40915](#)) has long been interested in fair division and is the author of three books on the subject, the latest being *Mathematics and Democracy: Designing Better Voting and Fair-Division Procedures* (Princeton University Press, 2008). He is Professor of Politics at New York University and works regularly with mathematicians, economists, and computer scientists on a variety of interdisciplinary topics.

D. MARC KILGOUR (MR Author ID: [101405](#)) is Professor of Mathematics at Wilfrid Laurier University in Waterloo, Canada. Beginning from a base in game theory, he works at the intersection of mathematics, engineering, and social science and has contributed on topics ranging from environmental management and decision support to electoral systems and fair division.

CHRISTIAN KLAMLER (MR Author ID: [730171](#)) is Associate Professor of Economics at the University of Graz in Austria. His research interests lie in the algorithmic and the normative analysis of fair-division procedures and voting rules.

Volume/Surface Area Ratios for Globes, with Applications

TOM M. APOSTOL

California Institute of Technology
Pasadena, CA 91125
apostol@caltech.edu

MAMIKON A. MNATSAKIAN

California Institute of Technology
Pasadena, CA 91125
mamikon@caltech.edu

A spectacular landmark in the history of mathematics was the discovery by Archimedes that the volume of a solid sphere is two-thirds the volume of the smallest right cylinder that surrounds it and that the surface area of the sphere is also two-thirds the total surface area of the same cylinder. Archimedes was so excited by this discovery that he wanted a sphere and its circumscribing cylinder engraved on his tombstone. He made this particular discovery by balancing slices of a sphere and cone against slices of a larger cylinder, with diameter twice that of the sphere, using centroids and the principle of the lever, which were also among his remarkable discoveries.

In [1], Chapter 5, a simple treatment of Archimedes's tombstone result was based on a family of solids called *Archimedean globes*.

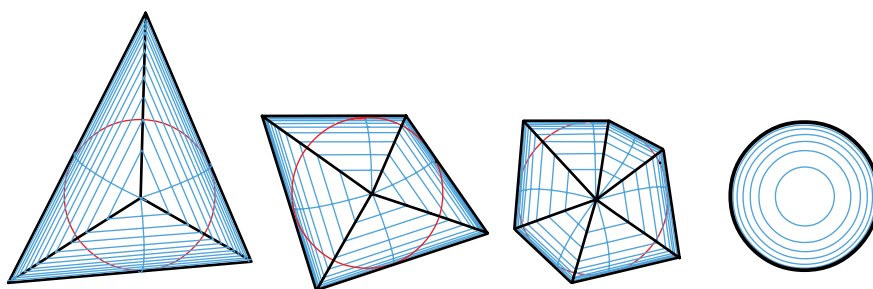


Figure 1 Archimedean globes (top view) showing equators for $n = 3, 4, 6$, and ∞ .

Cross sections of these globes by planes parallel to the equatorial plane are disks bounded by similar n -gons that circumscribe the circular cross sections of the insphere, as depicted by the examples in Figure 1. The volume of each globe is two-thirds the volume of its circumscribing prism (Theorem 5.3(b) of [1]), and the surface area of each globe is two-thirds the total surface area of its circumscribing prism (Theorem 5.7 of [1]). Therefore, the ratio volume/surface area of these globes is the same for each member of the family. This paper extends this remarkable property to more general globes in which the polygonal cross sections are replaced by similar circumgonal regions. Basic properties of circumgonal regions are described in the next section.

Fundamental properties of circumgonal regions

Figure 2 shows examples of building blocks of circumgonal regions. The right triangular region in Figure 2a is called a *wedge*; its *outer edge* is tangent to a circle called the *incircle*. Figure 2b is the union of two adjacent wedges whose tangential edges form one outer edge of a circumgon. Figure 2c is the set-theoretic difference of two wedges. It has an outer edge that does not touch the incircle but lies on a tangent line to the incircle. In Figure 2d the union of two congruent wedges forms a symmetric corner. Figure 2e, a sector of the incircle, is also considered a building block.

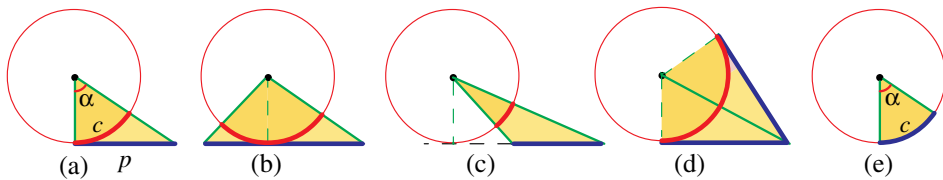


Figure 2 The shaded regions are building blocks of circumgonal regions.

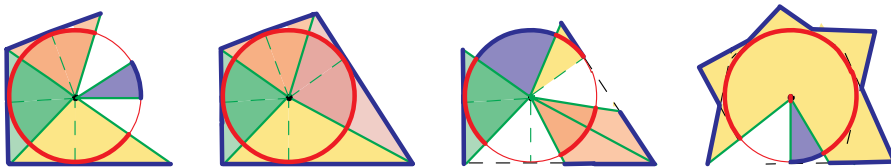


Figure 3 The shaded regions are examples of circumgonal regions.

In [1], p. 106, a *circumgonal region* is defined to be the union of a finite set of nonoverlapping building blocks that circumscribe a circle, called the *incircle*, whose radius is the *inradius*. The union of the corresponding outer edges, which may include circular arcs, is called a *circumgon*. Examples are shown in Figure 3, where the building blocks are shaded and the outer edges are shown with dark lines. The sum of the lengths of the outer edges is called the *perimeter* of the circumgon. This is not its perimeter in the usual Euclidean sense unless the circumgon is closed. This definition of perimeter leads to the following fundamental property that generalizes the relation between the area and perimeter of a circular disk:

The area of a circumgonal region is half the product of its perimeter and inradius.

This implies that for any two circumgonal regions with the same incircle, the ratio of their perimeters P_1/P_2 is equal to the ratio of their corresponding areas A_1/A_2 :

$$\frac{P_1}{P_2} = \frac{A_1}{A_2}. \quad (1)$$

Each building block contains a sector of the incircle. We define the *core* of a circumgonal region to be the union of all the sectors contained in its building blocks. Thus, the core is also a circumgonal region whose outer edges are the intercepted arcs of the incircle. In Figure 2e, the circumgonal region and its core are identical.

When the second circumgonal region in (1) is the core of the first circumgonal region, we denote the common ratio in (1) by the symbol ρ . Specifically, for a given circumgonal region, the ratio of its perimeter to that of its core is denoted by ρ .

Note that $\rho \geq 1$ and that ρ approaches 1 as the circumgon approaches the incircle. By (1), ρ is also the ratio of the area of a circumgonal region to that of its core.

As an example that will be used later, choose the circumgonal region and core to be the wedge and sector in Figure 2a. Let p denote the perimeter of the wedge and c the length of the arc. Then for this circumgonal region, we have

$$\rho = \frac{p}{c} = \frac{\tan \alpha}{\alpha}, \quad (2)$$

where α is the central angle of the arc. This is also the ratio of their areas. When the wedge is isosceles, we have $\alpha = \pi/4$ and $\rho = 4/\pi$.

Globes built from similar circumgonal regions

This section constructs three-dimensional *globes*, whose cross sections parallel to a given base plane are similar polygonal circumgonal regions, as suggested in Figure 4a. The base plane can be chosen through any circumgon with positive inradius. The incenters of the circumgonal cross sections are centers of similarity, and they lie on an axis perpendicular to the base plane. The scaling factor varies continuously, having the value 1 at the base plane.

The *core* of the globe is defined to be the union of all the planar cores of its circumgonal cross sections. The core is part of a solid of revolution. In particular, the core of an Archimedean globe is its insphere. The top view of a general globe will resemble the Archimedean globes in Figure 1. Each circumgonal region is made up of building blocks, and the globe is divided naturally by vertical planes through the axis into solid wedges having these building blocks as bases, examples of which are in Figures 4b, 4c, and 4d, the portion of each core being shaded. The globe is tangent to its core along the profile of a cylinder that forms a curved portion of the outer surface of each wedge. Because the core is part of a solid of revolution, all curved faces are portions of cylinders with the same profile.

Figure 5 shows how to construct a special globe whose horizontal cross sections are squares. The plane region in Figure 5a is rotated once around the axis to form the core in Figure 5b, a solid of revolution. Figure 5c shows a symmetric section of this core cut by a plane through the axis of revolution. Figure 5d shows a solid cylinder whose profile is the plane region in (c). Figure 5e shows the solid of intersection of two *orthogonal* cylinders of type (d) together with the solid of revolution in (b) that it circumscribes. This solid of intersection is a globe that was treated by Archimedes. A typical cross section of this globe cut by a horizontal plane (shown shaded in Figure 5e) is a square because the two cylinders are orthogonal. Each horizontal cross section of the core is a circular disk, the planar core of the square.

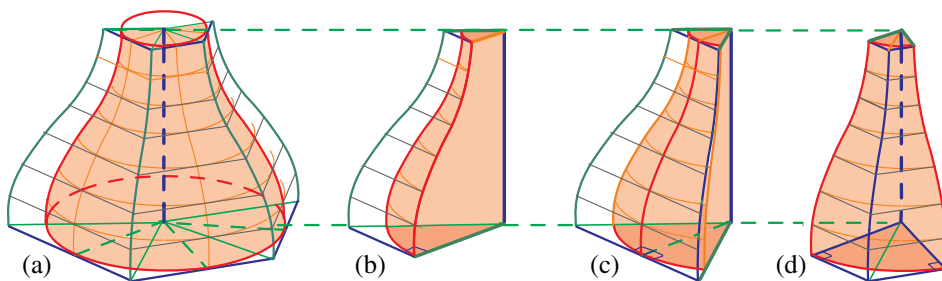


Figure 4 Globes whose cross sections are similar polygonal circumgonal regions.

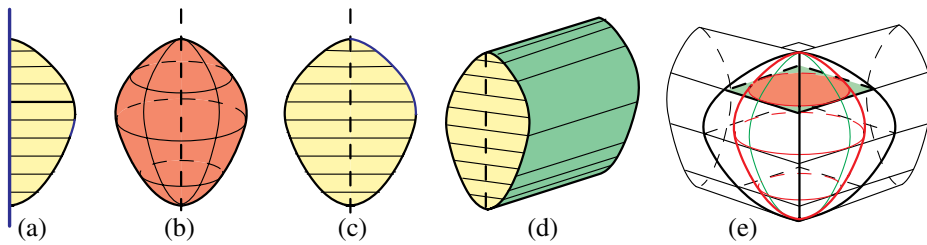


Figure 5 (a) Plane region rotated to form solid core in (b). (c) Axial cross section of (b). (d) Cylinder with profile (c). (e) Globe is solid of intersection of two orthogonal cylinders of type (d) circumscribing the core in (b).

In general, a globe is obtained as the solid of intersection of finitely many wedges formed by semicylinders of type (d) in Figure 5, as indicated in Figure 4a, in which case the square in Figure 5e is replaced by a circumgon, a polygon circumscribing a circular section of the core.

Volume and surface area relations for globes

This section begins with a surprising connection relating the volume of the special globe and that of its core in Figure 5. Figure 6a shows this globe G and its core C from Figure 5e, and three horizontal similar square circumgonal sections. Let $V(G)$ and $V(C)$ denote their respective volumes. We will show that

$$\frac{V(G)}{V(C)} = \frac{4}{\pi}. \quad (3)$$

As noted, the cross sections in Figure 6a are similar circumgonal regions, each of which is a square circumscribing a circular disk. A disk of radius r has area πr^2 ; its circumscribing square has area $4r^2$, so in every horizontal cross section of globe and core the constant ratio of areas, $A(\text{square})/A(\text{disk}) = 4/\pi$. Because each of $V(G)$ and $V(C)$ is the integral of cross-sectional areas, the ratio of volumes, $V(G)/V(C)$ is the same constant, and we obtain (3). By (1), $4/\pi$ is also the ratio $\rho = p/c$ of the perimeter of the square to the circumference of the incircle.

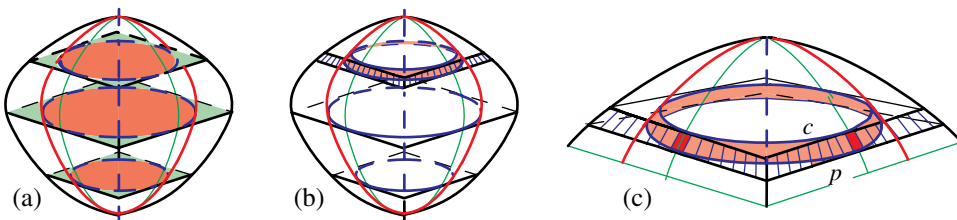


Figure 6 (a) Globe and inscribed core cut by horizontal planes showing similar circumgonal sections. (b) Thin zone of globe and its core cut by two planes. (c) Magnified view of (b).

It is even more surprising that this ρ is also the ratio of the surface area $S(G)$ of the globe to the surface area $S(C)$ of its core, so we have the following chain of equal ratios:

$$\frac{4}{\pi} = \rho = \frac{p}{c} = \frac{A(\text{square})}{A(\text{disk})} = \frac{S(G)}{S(C)} = \frac{V(G)}{V(C)}. \quad (4)$$

To prove $S(G)/S(C) = 4/\pi$, refer to Figure 6b, which shows a thin zone cut from the surfaces of the globe and its core by two nearby horizontal planes. The zone is magnified in Figure 6c. The surface of the shaded band of the core can be approximated by small rectangles of equal area, two of which are indicated by the darker shading. Because the globe is tangent to the core, the corresponding surface area of the globe can be approximated by small rectangles of the same type. It can be shown (details omitted) that the ratio of the two approximations, area of global zone to area of core zone, is equal to the ratio of the two perimeters, square to circle, which is the constant $4/\pi$. Consequently, the same constant ratio holds for the union of all the zones, and we deduce that $S(G)/S(C) = 4/\pi$. This proves (4) for globes formed by two *orthogonal* intersecting cylinders.

We note that the chain of ratios in (4) also holds if globe G and its core C are replaced by any slice cut by two horizontal parallel planes. This is because each such slice produces a new globe and its core. However, the outer surface of a slice consists of two parts, the lateral surface and the planar portions on the top and bottom lying in the cutting planes. The foregoing proof shows that the lateral surface areas of the sliced globe and core have the ratio ρ . The same is true, of course, for each planar face on top and bottom. Simple algebra shows that the ratio of areas of the total outer surfaces, lateral plus planar, is also equal to ρ . Consequently, when we refer to the ratio of surface areas, globe to core, the ratio is the same ρ , both for lateral surfaces and total outer surfaces, and is *independent of the thickness of the slice*!

The foregoing argument can be used to extend the relations in (4) to *arbitrary* globes and their cores. For each globe G and its core C , we denote, as above, their respective volumes by $V(G)$, $V(C)$ and their respective outer surface areas by $S(G)$, $S(C)$. We also introduce the notations $A(G)$ and $A(C)$ to denote the areas of the circumgonal cross sections of G and C , respectively. Again, let $\rho = p/c$, the ratio of perimeters, circumgon to core. Then we have the following surprising chain of equalities.

Theorem 1. *For any globe G and its core C we have*

$$\rho = \frac{p}{c} = \frac{A(G)}{A(C)} = \frac{S(G)}{S(C)} = \frac{V(G)}{V(C)}. \quad (5)$$

The last equality in (5) is equivalent to

$$\frac{V(G)}{S(G)} = \frac{V(C)}{S(C)}. \quad (6)$$

We note once more that Theorem 1 is valid for any slice of a globe and its core cut by two horizontal parallel planes because such a slice is also a globe. The surface area ratio in (5) is the same for both the lateral surfaces and total outer surfaces. As already noted, the ratio ρ is independent of the thickness of the slice.

Archimedean globes can also be constructed by combining wedge-like portions of n semicircular cylinders whose axes are in the equatorial plane and intersect at the center of the inscribed equator, each axis being parallel to an edge of the polygonal base. The two simplest examples formed from triangular and square circumgons are shown in Figure 7. In particular, when the core is a sphere, the globe is the solid of intersection of two circular cylinders considered by Archimedes (Figure 7b). He found the volume of this globe is two-thirds the volume of its circumscribing cube, but he did not treat its surface area, which, as shown in [1], Theorem 5.7, is also two-thirds that of the same cube.

The relation between volume and lateral surface area of an n -dimensional cylindrical wedge was discussed in [1], p. 428. By combining cylindrical wedges, as was done above, we can construct n -dimensional globes and their cores. This leads to an

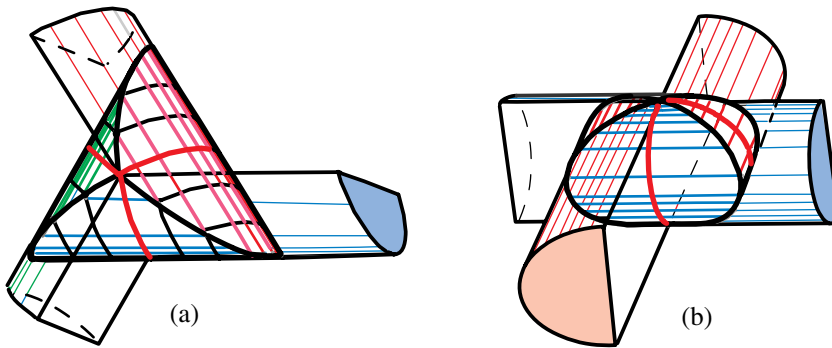


Figure 7 Portions of semicircular cylindrical wedges combined to form Archimedean globes.

extended chain of equal ratios like those in (5), each ratio being equal to the *fundamental ratio* ρ for the underlying circumgon and its core. As we advance from a given space to a space of one higher dimension, we *add two new equal ratios to the chain, one for surface areas and another for volumes*:

Theorem 2. For any n -globe G and its n -core C we have

$$\rho = \frac{S_n(G)}{S_n(C)} = \frac{V_n(G)}{V_n(C)}.$$

Theorem 3 extends Theorem 1 to higher-dimensional space.

When the core of an n -dimensional globe is an n -sphere, the globe is an Archimedean globe. The equality of ratios of volumes and outer surface areas of such globes and their cores also follows from Theorem 4.13 of [1]. In general, an n -globe can be regarded as a generalized circumsolid with the core playing the role of the insphere.

Theorem 3 implies the following important result relating two globes having the same core.

Theorem 3. For any two n -globes G_1 and G_2 having the same n -core C and respective fundamental ratios $\rho(1)$ and $\rho(2)$, we have

$$\frac{\rho(2)}{\rho(1)} = \frac{S_n(G_2)}{S_n(G_1)} = \frac{V_n(G_2)}{V_n(G_1)}.$$

An example illustrating Theorem 3 appears in Figure 8.

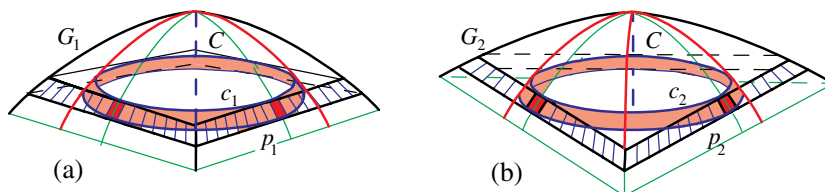


Figure 8 (a) Slice of globe G_1 with square base of perimeter p_1 . (b) Slice of the same thickness and same level of globe G_2 with triangular base of perimeter p_2 .

Figure 8a shows a slice of a globe G_1 with a square base of perimeter p_1 , and Figure 8b shows a slice of the same thickness and at the same horizontal level of a globe G_2 with a triangular base of perimeter p_2 . The globes have a common core C ,

and the quotient of fundamental ratios $\rho(2)/\rho(1)$ in this case is equal to p_2/p_1 because the two incircle perimeters c_2 and c_1 are equal.

Examples of square-based globes Figure 9 shows a family of circumsolids of revolution of height $2r$, including the limiting case of the insphere, all having equal lateral surface area, which is that of the circumscribing cylinder, $4\pi r^2$. The number below each image indicates the number of sides of the regular polygon rotated to form the circumsolid.

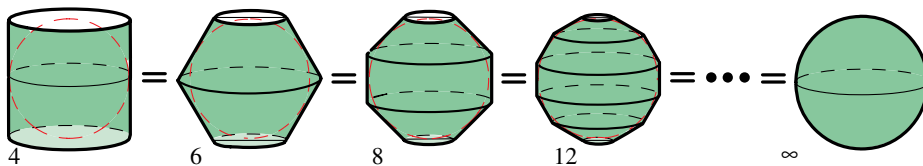


Figure 9 Circumsolids of revolution of equal lateral surface areas used as cores.

Figure 10 shows a family of punctured circumsolids of revolution of height $2r$ having the same volume as the insphere and its punctured circumscribing cylinder, $4\pi r^3/3$. These solids of revolution were discussed in [1], Figures 13.9 and 13.14.

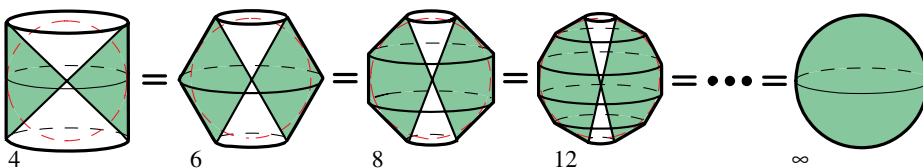


Figure 10 Punctured circumsolids of revolution of equal volumes used as cores.

Figure 11 shows two families of square-based globes.

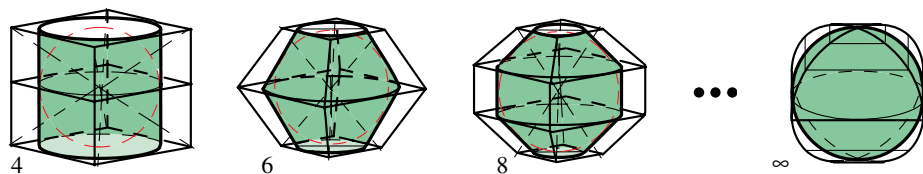


Figure 11 Square-based globes with circumsolids of revolution as cores.

One family (unpunctured) has the cores in Figure 9, and the other (punctured) has the cores in Figure 10.

We shall apply Theorem 1 to the entire family of square-based globes in Figure 11. Each family of globes in Figure 11 inherits the equality of lateral surface areas from Figure 9 and the equality of volumes from Figure 10.

Applying Theorem 1 for square-based globes, for which $\rho = 4/\pi$, we see that, in all these examples (punctured or unpunctured), relation (5) holds *not only for the lateral surface areas but also for the surface areas obtained by including one or both bases*. All the punctured square-based globes have equal lateral surface areas $16r^2$ and equal volumes $16r^3/3$.

Application to elliptic cylindrical wedge

This section applies Theorem 1 to calculate the surface area of an elliptic cylindrical wedge regarded as a globe. An example of such a wedge is obtained by uniform dilation of a circular cylindrical wedge forming a component of an Archimedean globe. The dilation takes place along the axis perpendicular to the equatorial plane.

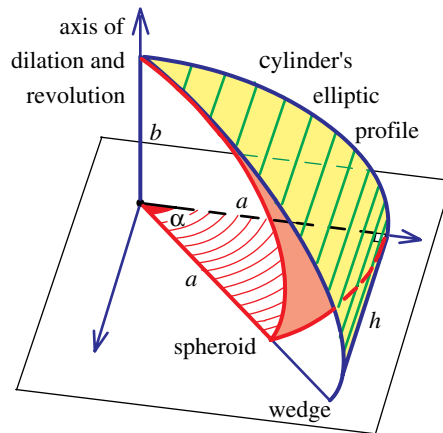


Figure 12 Elliptic wedge as a globe with a spheroidal sector as its core.

In Figure 12, the circumgonal base is a right triangle with vertex angle α at the center of the incircle of radius a . Dilation by a factor b/a produces an elliptic cylindrical wedge of edge length $h = a \tan \alpha$ at the base. The cylindrical profile of the wedge is a semiellipse with semi axes a and b . The outer cylindrical surface is indicated by parallel line segments. The core of this globe is a sector of a spheroid (an ellipsoid of revolution around the dilation axis) with equatorial radius a , whose lateral surface is shown shaded.

When a sphere or spherical wedge is dilated by a factor λ to obtain a spheroid or a spheroidal wedge, its volume is multiplied by the dilation factor λ , but its surface area is multiplied by a more complicated factor involving the eccentricity of the elliptic profile (see [3]). In any case, both the volume and surface area of the spheroid or spheroidal wedge can be considered as known. The elliptical wedge in Figure 12 is a globe having a spheroidal wedge as its core. By Theorem 1, the lateral surface area of this globe is simply ρ times that of its core, where $\rho = (\tan \alpha)/\alpha$ by (2). In terms of the edge length h of the wedge and inradius a , we now have $\rho = h/(a\alpha)$. To the best of our knowledge, the lateral surface area of an elliptic cylindrical wedge has not been previously recorded in the literature.

Volume/surface area ratios for spheroid and sinoid

The surface area of a spheroid can be calculated by using integral calculus. This section gives an alternate calculation that is much simpler. It relates the area of a spheroid to that of another solid we call a *sinoid* (pronounced *sine oid*) obtained by rotating the ordinate set of a sine curve. In Figure 13a, a slanted plane through the diameter of the base of a circular cylinder cuts the lateral surface of the cylinder along an ellipse. When this ellipse is rotated around the diameter, it generates a spheroid (Figure 13b). Now unwrap the lateral surface of the cylinder onto a plane. The unwrapped ellipse

becomes a sine curve (see [1], Sec. 6.2) that, when rotated around a horizontal x axis, generates the surface of a sinoid, as shown in Figure 13c.

We were surprised to find that *the surface area of the sinoid is equal to that of the spheroid times the eccentricity of the ellipse*.

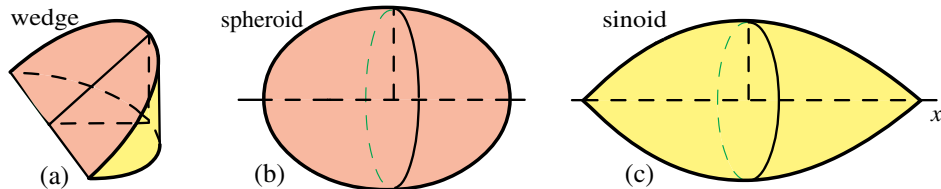


Figure 13 Surface areas of spheroid and sinoid related by the eccentricity of the ellipse.

We shall derive this from a more general result described below in which the cylinder is not necessarily circular. But first, we note that this gives us a simple alternate calculation of the surface area of a spheroid. The surface area of a sinoid is easily found by integral calculus. Dividing this by the eccentricity of the ellipse yields the surface area of the spheroid. Even more surprising, the same ratio of areas, sinoid to spheroid, also holds for corresponding zones of the sinoid and spheroid. We will prove this for the more general solids shown in Figure 14.

Figure 14a shows a wedge generalizing that in Figure 13a. It is cut from a cylinder, not necessarily circular, by a plane inclined at angle α passing through the base of the cylinder. The cutting plane intersects the lateral surface of the cylinder along a curve that, when rotated about the line of intersection of the cutting plane and base, produces the outer surface of a spheroid-like solid, as indicated in Figure 14b. When the lateral surface of the cylinder in Figure 14a is unwrapped onto a plane it fills a region that, when rotated around the x axis, produces a sinoid-like solid like that in Figure 14c, generalizing the sinoid in Figure 13c.

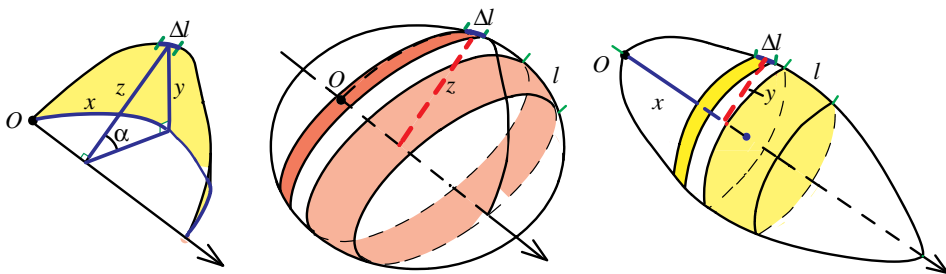


Figure 14 The ratio of surface areas of a sinoid-like solid and a spheroid-like solid is $\sin \alpha$.

To relate their surface areas, refer to a typical vertical cross section of the wedge in Figure 14a, a right triangle of height y and hypotenuse z , with $y = z \sin \alpha$. When a small arc of length Δl is rotated around the axis indicated by the arrow, it generates an element of the spheroid-like surface (shown with dark shading in Figure 14b) whose area, by Pappus's theorem, is $2\pi z \Delta l$. The length of arc Δl is preserved by unwrapping from Figure 14a to 14c, so when the unwrapped arc of length Δl in Figure 13c is rotated about the x axis it generates a corresponding element of the sinoid-like surface whose area is $2\pi y \Delta l$. The ratio of areas of these surface elements, sinoid-like

to spheroid-like, is $y/z = \sin \alpha$, a constant independent of the location of the vertical cross section, so the same ratio also holds for surfaces that are the union of such elements, for example, corresponding zones of the two surfaces cut by parallel planes that intercept the same length l of arc as indicated in Figures 14b and 14c. In particular, for the full surfaces the area ratio is $\sin \alpha$. Finally, we note that for the special case shown in Figure 13, the ratio $\sin \alpha$ is the eccentricity of the ellipse, which yields the result for areas asserted earlier.

The result for the solids in Figure 13 can be expressed as follows. Let $S(\text{sinoid})$ and $S(\text{spheroid})$ denote the lateral surfaces of the sinoid and spheroid in Figures 13c and 13b, respectively. We have shown that

$$\frac{S(\text{sinoid})}{S(\text{spheroid})} = e, \quad (7)$$

where $e = \sin \alpha$ is the eccentricity of the ellipse in Figure 13a. The corresponding volumes of these solids are known to be $V(\text{sinoid}) = \frac{1}{2}\pi^2 r^3 \tan^2 \alpha$ and $V(\text{spheroid}) = \frac{4}{3}\pi r^3 / \cos^2 \alpha$, where r is the radius of the circular cylinder in Figure 13a, which gives the ratio

$$\frac{V(\text{sinoid})}{V(\text{spheroid})} = \frac{3\pi}{8} e^2. \quad (8)$$

Thus, we have

$$\frac{V(\text{sinoid})}{S(\text{sinoid})} = \frac{3\pi}{8} e \frac{V(\text{spheroid})}{S(\text{spheroid})}. \quad (9)$$

It is worth mentioning that the wedge in Figure 13a is only one member of an infinite family of circumgonal wedges of equal volume and equal lateral surface areas, described in Figures 13.16 and 13.17 in [1]. Their cylindrical bases are halves of regular $2n$ -gons. A plane inclined at angle α intersects each wedge along a polygonal curve circumscribing a semiellipse. An example with $n = 6$ is shown in Figure 15a.

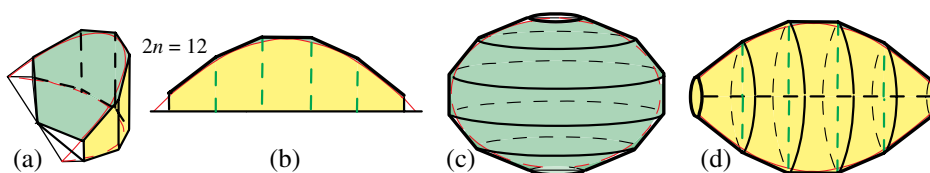


Figure 15 The ratio of lateral surface area of solid circumscribing sinoid in (d) to that of the solid circumscribing spheroid in (c) is the eccentricity of the inscribed ellipse in (a).

When each such curve is rotated around the line of intersection it produces a solid of revolution, a dilated version of those in Figure 9, each of which circumscribes a spheroid (Figure 15c). Moreover, when the corresponding unwrapped lateral surface of the wedge (Figure 15b) is rotated about its horizontal base it produces a solid of revolution circumscribing a portion of a sinoid (Figure 15d). For every n the lateral surface area of this solid is related by (7) to the corresponding surface area in Figure 10. Relations (8) and (9) also hold for the extreme cases $n = 2$ and $n = \infty$. And for intermediate values of n they hold with the coefficient $3\pi/8$ replaced by a factor that varies slightly with n .

In Figure 16a, P denotes a section of the wedge cut by an arbitrary vertical plane perpendicular to the base diameter of the wedge. Two such planes generate a zonal

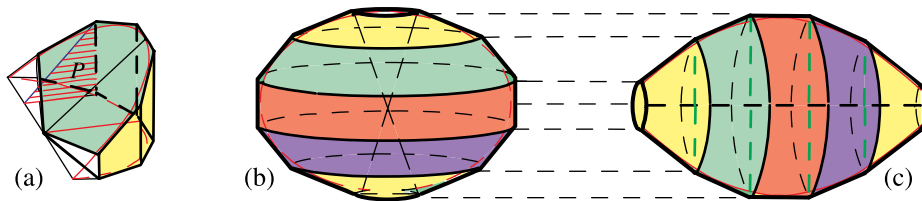


Figure 16 Each zonal slice on a spheroid in (b) and its corresponding zonal slice on a sinoid in (c) satisfy the relations in Equations (7) through (9).

slice on the spheroid in Figure 16b and a corresponding zonal slice (with the same shading) on the sinoid in Figure 16c. Formulas (7), (8) and (9) are also valid for these corresponding zonal slices. In Figure 16a, P passes through a vertex of the wedge. But the final result holds for zonal slices generated by any two parallel planar sections P because the portion of the circumgonal base of the wedge cut off by these planes is also a circumgon. We were pleasantly surprised to find that this result is analogous to that in Theorem 1 of [2].

REFERENCES

1. T. M. Apostol and M. A. Mnatsakanian, *New Horizons in Geometry*. Dolciani Mathematical Expositions No. 47, Mathematical Association of America, 2012.
2. T. M. Apostol and M. A. Mnatsakanian, Volume/surface area relations for n -dimensional spheres, pseudo-spheres, and catenoids. *Amer. Math. Monthly*, **122** (2015) 745–756.
3. <http://en.wikipedia.org/wiki/Spheroid>

Summary. We introduce families of solids called globes, having an invariant ratio of volume to surface area. An application determines the lateral surface area of an elliptical wedge in terms of its volume. We also relate surface areas and volumes of corresponding zonal slices of a spheroid and sinoid via the eccentricity of an ellipse.

TOM M. APOSTOL (MR Author ID: [26600](#)) joined the Caltech faculty in 1950 and became professor emeritus in 1992. He is director of *Project MATHEMATICS!* (<http://www.projectmathematics.com>), an award-winning series of videos he initiated in 1987. His long career in mathematics is described in the September 1997 issue of *The College Mathematics Journal*. He was selected as a Fellow of the American Mathematical Society in 2012. He is currently working with colleague Mamikon Mnatsakanian to produce materials demonstrating Mamikon's innovative and exciting approach to mathematics.

MAMIKON A. MNATSAKANIAN (MR Author ID: [247531](#)) received a Ph. D. in physics in 1969 from Yerevan University, where he became a professor of astrophysics. As an undergraduate, he began developing innovative geometric methods for solving many calculus problems by a dynamic and visual approach that makes no use of formulas. He is currently working with Tom Apostol under the auspices of *Project MATHEMATICS!* to present his methods in a multimedia format.

Coming soon in the *College Mathematics Journal*

Yet More Ways to Skin a Definite Integral by *Brain Bradie*

Area and Perimeter Bisecting Lines of a Triangle by *Allan Berele and Stefan Catoiu*

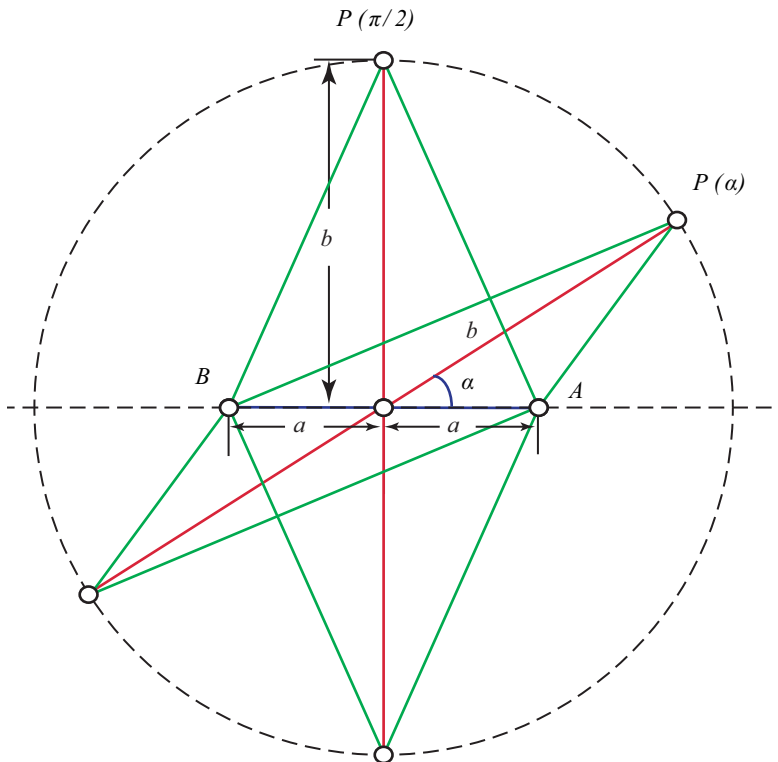
The Parallelogram with Maximum Perimeter for Given Diagonals Is the Rhombus—A Proof Without Words and a Corollary

ANGEL PLAZA

Universidad de Las Palmas de Gran Canaria
Las Palmas, Spain
angel.plaza@ulpgc.es

Theorem. *The parallelogram with maximum perimeter for given diagonals is the rhombus.*

Proof.

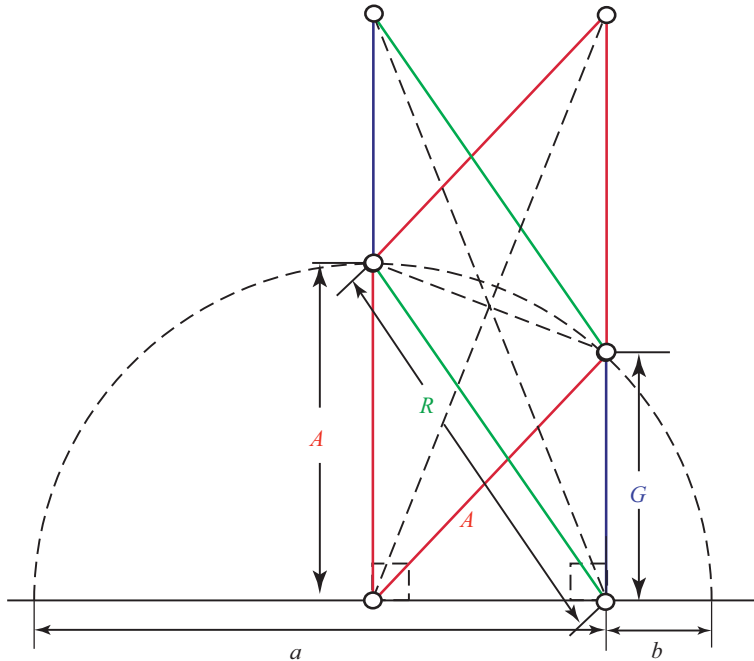


$$|AP(\alpha)| + |BP(\alpha)| = \sqrt{a^2 + b^2 - 2ab \cos \alpha} + \sqrt{a^2 + b^2 + 2ab \cos \alpha} \\ \leq 2\sqrt{a^2 + b^2}$$

(by the Law of Cosines and the arithmetic mean-root mean square inequality).

Corollary. *For two positive numbers a and b , let us denote by A , G , and R , respectively their arithmetic mean, geometric mean, and root mean square, then $2A \geq R + G$.*

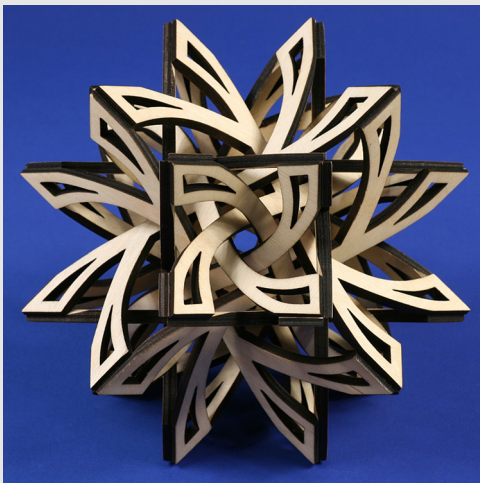
Proof.



(where two parallelograms with equal diagonals have been constructed from the geometric representation of the arithmetic mean, geometric mean, and root mean square of two positive given numbers).

Summary. By the Law of Cosines and the arithmetic mean-root mean square inequality it is proved without words that The Parallelogram with Maximum Perimeter for given Diagonals is the Rhombus. As a corollary it also proved that for two positive numbers, their arithmetic mean is greater or equal than the arithmetic mean of their geometric mean and their root mean square.

ANGEL PLAZA (MR Author ID: [350023](#)) received his masters degree from Universidad Complutense de Madrid in 1984 and his Ph.D. from Universidad de Las Palmas de Gran Canaria in 1993, where he is a Full Professor in Applied Mathematics. He is interested in mesh generation and refinement, combinatorics and visualization support in teaching and learning mathematics.



Artist Spotlight George Hart

Dragonflies, George Hart; wood, 7.5 inches in diameter, 2009; private collection. Constructed from 12 identical plywood components.

See interview on page 374.

ACROSS

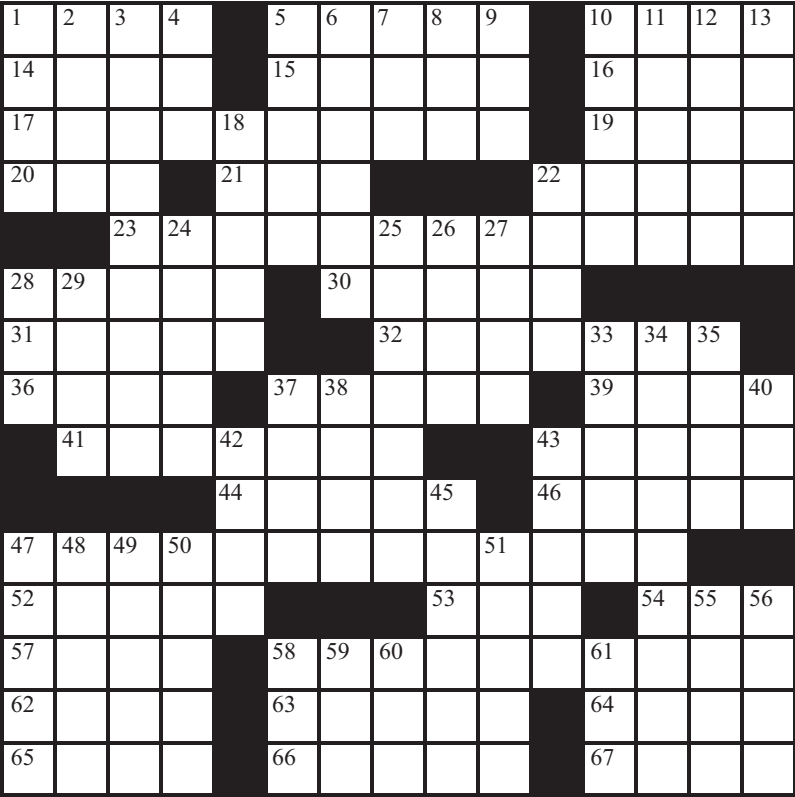
1. A theorem in functional analysis features his name, along with Banach
5. Slang term for criminals
10. * Statistician Xiao-Li whose invited address is about big data
14. Part of a nursery rhyme: "... wish ____, wish ..."
15. Text editor originally written by Richard Stallman and Guy Steele
16. Asia's ____ Sea
17. * American algebraist who is giving the Association for Women in Mathematics' Noether Lecture
19. "The ____ Book," popular math book by Simon Singh
20. Conclude
21. Acute cystitis: Abbr.
22. ____ of attraction: region of phase in which any point will eventually be iterated to the system's attractor
23. * British Fields Medalist who is giving an invited colloquium lecture on quasirandom graphs
28. Nuclear weapon: Hyph.
30. Modern auto company named for a famous physicist/engineer
31. "Love Shack" lyrics: "I got me a car . . . ____ a whale"
32. * Location of JMM 2016
36. Remnant at the bottom of a mug
37. Quark flavor
39. Harvest
41. Sound systems
43. "Yeah, right!"
44. It can mean "hello" or "goodbye"
46. { } : the ____ set
47. * American mathematician whose MAA Lecture for Students is about fractal geometry
52. Poet Pound and musician Koenig
53. * One host of JMM
54. 2^x is this type of fn.
57. $f(x) = x^2 - x - 1$ has one at $x = \phi$
58. * Mathematician and humorist who is hosting Mathematically Bent Theater with his Mobiusbandaid Players
62. Years, in Latin
63. $\div \div \div \div \div$
64. Loads from lodes
65. * Project ____, MAA professional development program hosting several activities
66. Painters' canvases may come preprimed with this
67. "____ She Lovely?"

DOWN

1. Scouting outing
2. ____ for *All Seasons*, famous 1960 play
3. One way to play?
4. He's the Science Guy
5. Basil-based sauce
6. Former NFL star running back (with the same last name as 17 Across)
7. Honorific title in India, or a form of folk music that originated in Algeria
8. %: Abbr.
9. Remote login protocol: Abbr.
10. Long-tailed parrot
11. Jagged, as a leaf's edge
12. Rock bottom
13. Singers Campbell and Hansard
18. Deadens the pain, perhaps
22. Dinghy or dory
24. Given a function f and a subset X of f 's domain, it's the set of all outputs $f(x)$, where x comes from X
25. In *Mrs. Doubtfire*, it's what Robin Williams' character's son exclaims upon discovering his true identity
26. Belgian River that was the site of a WWI battle
27. ____ rock: subgenre typified by David Bowie, T. Rex, and Lou Reed
28. Possible status of a soon-to-be Ph.D.
29. North American institute for mathematics established in Alberta, CA in 2003
33. "Bring it on"
34. 2016 and 2000, for example, but not 1900
35. On a compass, it corresponds to $\theta = 0$
37. Member of a certain Indo-European people
38. Piece of safety equipment for handling noxious chemicals
40. Korean singer whose video was the first to reach 1 billion views on YouTube
42. Compressed archive files on Windows
43. The brainy bunch
45. Takes advantage of, as a resource
47. Showed again on TV
48. Layer with a hole
49. With "The," one of the five boroughs
50. Weird Al Yankovic parody of a Michael Jackson hit
51. Prenatal test, for short
55. Superhero group whose leader is a professor
56. "Hey, over here!"
58. Gearwheel
59. Award bestowed by Queen Eliz.
60. Guitar master Paul
61. "And how!"

Joint Mathematics Meetings 2016

BRENDAN W. SULLIVAN
Emmanuel College
Boston, MA 02115
sullivanb@emmanuel.edu



Clues start at left, on page 362. The Solution is on page 373.

Extra copies of the puzzle can be found at the MAGAZINE's website, www.maa.org/mathmag/supplements.

Crossword Puzzle Creators

If you are interested in submitting a mathematically themed crossword puzzle for possible inclusion in MATHEMATICS MAGAZINE, please contact the editor at maj@ams.org.

The Focus Locus Problem and Toric Sections

MICHAEL GAUL

North Seattle College
mgaul@northseattle.edu

FRED KUCZMARSKI

Shoreline Community College
fkuczmar@shoreline.edu

In 1680, just seven years before Newton published his proof that the planets orbit the sun in elliptical orbits, the astronomer Giovanni Cassini proposed that the orbits belonged to another family of curves. These curves, today called Cassini ovals, are similar to ellipses in their definition. Fix two *focal points* F_1 and F_2 , a distance $2a$ units apart. Each constant $b > 0$ gives a Cassini oval, defined as the set of points P in the plane such that $PF_1 \cdot PF_2 = b^2$. The ratio a/b , what we call the *eccentricity*, determines the shape of the oval. Figure 1 shows a family of confocal Cassini ovals with *semifocal length* $a = 1$.

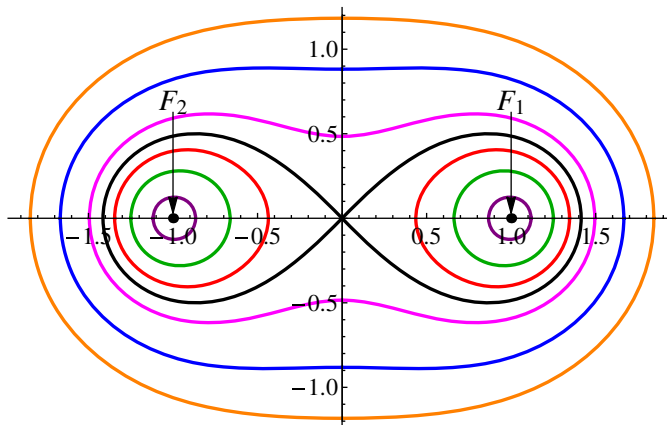


Figure 1 A family of confocal Cassini ovals.

Bernoulli's lemniscate is the figure-8 shaped curve in Figure 1; it is the Cassini oval with unit eccentricity. It is probably named after both Jacob and Johannes, as they each independently discovered the curve as the solution to a rather obscure problem in dynamics [1]. Neither recognized it as a Cassini oval [4].

The Cassini ovals belong to a broader family of curves, the spiroc sections of Perseus; these are cross sections of a torus cut by a plane parallel to its axis of symmetry. Generate a torus by rotating a circle of radius r about an axis in the plane of the circle, R units from its center. The spiroc section cut by a plane r units from the axis is a Cassini oval with semifocal length R [2, p. 18] and eccentricity $\sqrt{R/2r}$ (exercise). Choosing $R = 2r$ gives Bernoulli's lemniscate (Figure 2). If the cutting plane is $R - r$ units from the axis, tangent to the "inner ring" of the torus, the cross section is known as a lemniscate of Booth.

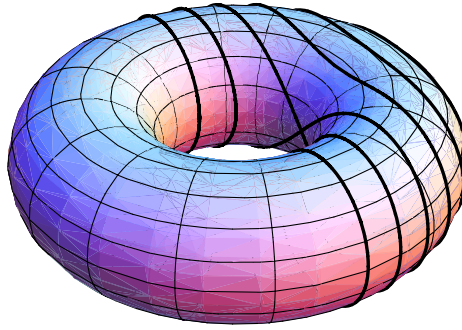


Figure 2 Bernoulli's lemniscate and other spiric sections.

The Booth lemniscates belong to yet another family, the Watt curves. James Watt included in his 1784 patent application for the steam engine a description of a three-bar linkage, designed to convert rotary motion into linear motion. The two outer bars AA' and BB' have equal lengths and are pinned at A and B (Figure 3). As these bars rotate freely about their endpoints, the midpoint M of the middle bar traces out a Watt curve. If $AB = A'B' > AA'$, the curve is a lemniscate of Booth. Choosing $A'B' = \sqrt{2}AA'$ gives Bernoulli's lemniscate.

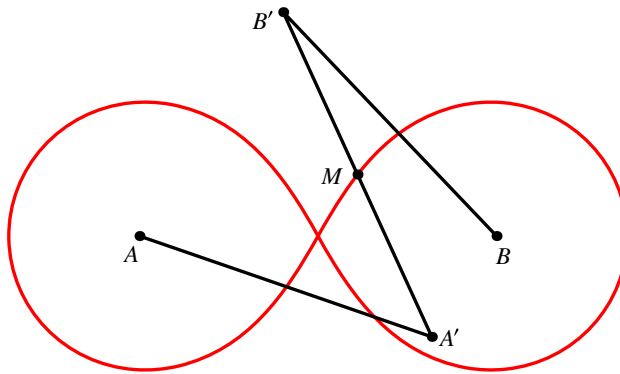


Figure 3 A lemniscate of Booth as a Watt curve.

While there are yet other ways to describe the lemniscates, we were surprised to see both the Cassini ovals and the lemniscates of Booth come up in our consideration of the following problem. Start with a unit circle C^+ in the xz -plane, centered at $(0, 0, 1)$. Fix a vector $\mathbf{v}_{\phi, \theta} = \langle \cos \theta \cos \phi, \sin \theta \cos \phi, -\sin \phi \rangle$, with $\phi \neq 0$. Consider the *parallel projection*, $\Pi_{\phi, \theta}$, that maps each point P of the xz -plane to the intersection point P' of the xy -plane and the line through P parallel to $\mathbf{v}_{\phi, \theta}$ (Figure 4). We like to think of P' as the shadow cast by P onto the xy -plane by an infinitely distant light source in the direction of $-\mathbf{v}_{\phi, \theta}$. The shadow of C^+ under this projection is an ellipse. Our problem is the following.

The Focus Locus Problem. For fixed $\phi \in (0, \pi/2)$, describe the path traced by the foci of the elliptical shadows $\Pi_{\phi, \theta}(C^+)$, as θ ranges from 0 to 2π .

This path, the ϕ -focus locus, depends on the inclination ϕ of the vector $\mathbf{v}_{\phi, \theta}$. This is the angle that $\mathbf{v}_{\phi, \theta}$ makes with the xy -plane. You might wish to pause here and try to visualize the $\pi/4$ -focus locus.

Bernoulli's lemniscate and the Cassini ovals

Since a parallel projection maps the center of a circle to the center of its elliptical image, for fixed ϕ the centers of the ellipses $\Pi_{\phi,\theta}(\mathcal{C}^+)$ lie on a circle centered at the origin. To remove this complexity, we first consider a modified problem and determine the ϕ -focal path generated by the shadows of the unit circle \mathcal{C} , centered at the origin and lying in the xz -plane. These elliptical shadows are centered at the origin.

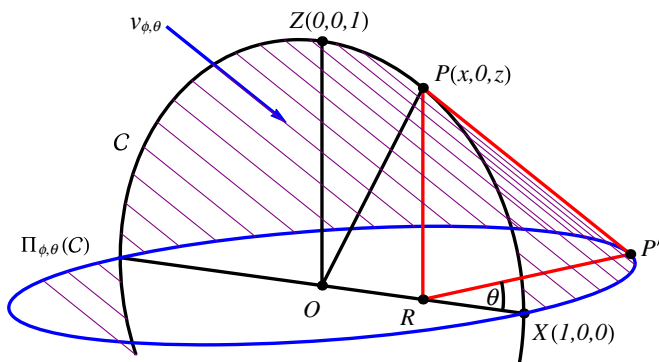


Figure 4 A parallel projection $\Pi_{\phi,\theta}$ to the xy -plane, $\phi = \pi/4$.

We start with $\phi = \pi/4$. The projection $\Pi_{\pi/4,\theta}$ maps the point $P(x, 0, z)$ in the xz -plane to the point $P'(x + z \cos \theta, z \sin \theta, 0)$ in the xy -plane. To see why, consider Figure 4, where $R(x, 0, 0)$ is the foot of the perpendicular from $P(x, 0, z)$ to the x -axis. Since $RP' = RP$ and $m\angle P'RX = \theta$,

$$\overrightarrow{OP'} = \overrightarrow{OR} + \overrightarrow{RP'} = \langle x, 0, 0 \rangle + \langle z \cos \theta, z \sin \theta, 0 \rangle.$$

By ignoring the y -coordinate of P and the z -coordinate of P' , we may regard the parallel projection as a linear transformation $T_\theta : \mathbb{R}^2 \rightarrow \mathbb{R}^2$, where

$$T_\theta \left(\begin{bmatrix} u \\ v \end{bmatrix} \right) = \begin{bmatrix} 1 & \cos \theta \\ 0 & \sin \theta \end{bmatrix} \begin{bmatrix} u \\ v \end{bmatrix}. \quad (1)$$

It is helpful to keep the three-dimensional nature of the our problem in mind, but we now replace our problem with an equivalent one in two dimensions. Let \mathcal{U} denote the unit circle in the uv -plane. Then the image of \mathcal{U} under T_θ coincides with the shadow of \mathcal{C} . To find the foci of this image, and hence those of the shadow, we first solve a more general problem and find the foci of $T(\mathcal{U})$ for any linear transformation $T : \mathbb{R}^2 \rightarrow \mathbb{R}^2$. To do so, we replace \mathbb{R}^2 with the complex plane and appeal to two facts.

- (a) A linear transformation of \mathbb{R}^2 can be represented as a function $f : \mathbb{C} \rightarrow \mathbb{C}$ of the form $f(z) = pz + q\bar{z}$, where $z = u + iv$ and $p, q \in \mathbb{C}$.
- (b) The image of \mathcal{U} under the map $w = f(z)$ is an ellipse with foci $\pm 2\sqrt{pq}$.

We leave the proof of (a) as an exercise, but point out that f gives a linear transformation of \mathbb{R}^2 since $z \rightarrow \bar{z}$ is a reflection in the real axis, and $z \mapsto pz$ is the composition of a rotation (by the angle $\arg(p)$) and a dilation (by the factor $|p|$) about the origin.

It is possible to give an algebraic proof of (b) [6], but we prefer a more geometric approach, modulo the assumption that the image is an ellipse \mathcal{E} centered at the origin o . Parameterize \mathcal{U} as $z = e^{i\alpha}$, $\alpha \in [0, 2\pi]$, and its image \mathcal{E} as

$$w = f(\alpha) = pe^{i\alpha} + qe^{-i\alpha}, \quad \alpha \in [0, 2\pi].$$

As α increases, $pe^{i\alpha}$ and $qe^{-i\alpha}$ rotate about the origin at equal rates, but in opposite directions, around circles of radii $|p|$ and $|q|$ respectively (Figure 5). Since $|f(\alpha)|$ is maximized when $pe^{i\alpha}$ and $qe^{-i\alpha}$ are parallel, the major axis of \mathcal{E} bisects $\angle poq$. Thus the foci of \mathcal{E} are *real* multiples of \sqrt{pq} (since $\arg(\sqrt{pq}) = (\arg(p) + \arg(q))/2$). Since the semimajor and semiminor axes have lengths $|p| + |q|$ and $||p| - |q||$ respectively, the semifocal length is

$$\sqrt{(|p| + |q|)^2 - (|p| - |q|)^2} = 2\sqrt{|pq|},$$

and (b) follows.

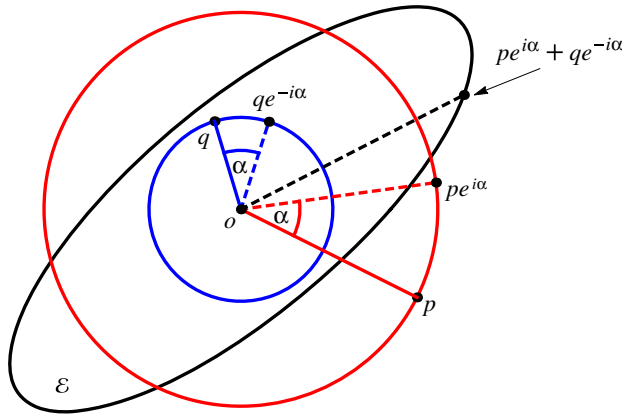


Figure 5 Finding the foci. Figure adapted from [5, p. 242].

One minor point. If f is not invertible, \mathcal{E} is a segment (or a point). But we may regard a segment as a degenerate ellipse with the endpoints as foci. The argument above shows that the endpoints of the segment are $\pm 2\sqrt{pq}$, and (b) still holds.

To use (b) to determine the foci of $T(\mathcal{U})$ under an arbitrary linear transformation $T : \mathbb{R}^2 \rightarrow \mathbb{R}^2$, let $f : \mathbb{C} \rightarrow \mathbb{C}$ correspond to T . Since

$$f^2(1) + f^2(i) = (p + q)^2 + (pi - qi)^2 = 4pq,$$

the foci are at $z = \pm\sqrt{f^2(1) + f^2(i)}$. They are the preimages of $w = f^2(1) + f^2(i)$ under the squaring map $z \mapsto w = z^2$.

We can now determine the $\pi/4$ -focus locus generated by \mathcal{C} ; this is the path traced by the foci of the ellipses $\Pi_{\pi/4, \theta}(\mathcal{C})$, for $\theta \in [0, 2\pi]$. But it is also the path traced by the foci of the ellipses $T_\theta(\mathcal{U})$, for $\theta \in [0, 2\pi]$. So let $f_\theta : \mathbb{C} \rightarrow \mathbb{C}$ correspond to the linear transformation T_θ . Since $f_\theta(1) = 1$ and $f_\theta(i) = e^{i\theta}$, the focus locus is the curve

$$z = g_\pm(\theta) = \pm\sqrt{f^2(1) + f^2(i)} = \pm\sqrt{1 + e^{2i\theta}}, \quad 0 \leq \theta \leq 2\pi, \quad (2)$$

where g_\pm denotes the two functions, g_+ and g_- , defined by (2). The focus locus is the preimage of the circle $w = 1 + e^{2i\theta}$ under $z \mapsto w = z^2$. But since

$$|g_\pm(\theta) + 1| |g_\pm(\theta) - 1| = |g_\pm^2(\theta) - 1| = |e^{2i\theta}| = 1,$$

the focus locus is Bernoulli's lemniscate with foci $z = \pm 1$.

To recover its more familiar polar equation, note that the lemniscate (2) is also generated for $\theta \in [-\pi/2, \pi/2]$. For these values of θ , $\cos \theta \geq 0$, and

$$g_\pm(\theta) = \pm\sqrt{1 + e^{2i\theta}} = \pm\sqrt{2 \cos \theta} e^{i\theta/2}.$$

By letting $\alpha = \theta/2$ denote the polar angle and r the polar radius this gives

$$r^2 = 2 \cos 2\alpha, \quad -\pi/4 \leq \alpha \leq \pi/4 \quad (3)$$

as the polar equation of Bernoulli's lemniscate.

Figure 6 shows some of the elliptical shadows cast by \mathcal{C} and suggests the motion of the foci along the lemniscate as θ increases at a constant rate. When $\theta = 0$, the vector $\mathbf{v}_{\pi/4, \theta}$ is parallel to the xz -plane and the shadow is a segment, a degenerate ellipse with foci $(\pm\sqrt{2}, 0)$. As θ increases, the foci move into the first and third quadrants as they speed up on their way toward the origin. They collide there when $\theta = \pi/2$ and the shadow is a circle. But rather than pass smoothly through the origin, the foci abruptly turn 90° and shoot into the second and fourth quadrants. We say *shoot* because the foci do not come to a stop as an actual particle must when it abruptly changes direction. Rather, their speeds tend toward infinity as they approach the origin.

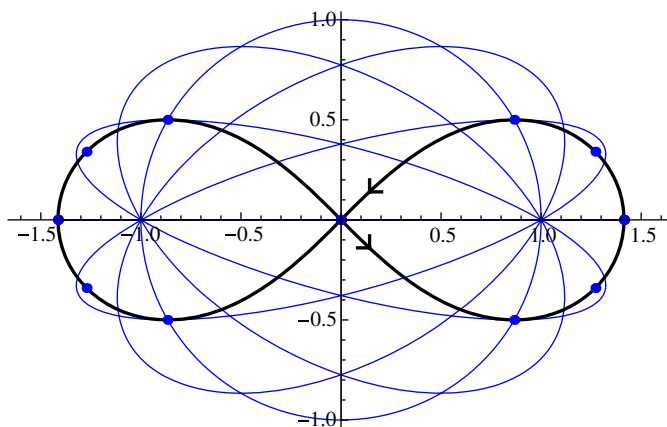


Figure 6 The family of elliptical shadows $\Pi_{\phi, \theta}(\mathcal{C})$ and their foci, $\phi = \pi/4$.

We now consider a general angle of inclination ϕ . Let $f_{\phi, \theta} : \mathbb{C} \rightarrow \mathbb{C}$ be the linear transformation corresponding to the parallel projection $\Pi_{\phi, \theta}$. This projection fixes $(1, 0, 0)$ and maps $(0, 0, 1)$ to $(\cot \phi \cos \theta, \cot \phi \sin \theta, 0)$. Hence, the ϕ -focus locus generated by \mathcal{C} is the curve

$$z = j_{\pm}(\theta) = \pm \sqrt{f_{\phi, \theta}^2(1) + f_{\phi, \theta}^2(i)} = \pm \sqrt{1 + \cot^2 \phi e^{2i\theta}}, \quad 0 \leq \theta \leq 2\pi. \quad (4)$$

It is the preimage of the circle $w = 1 + \cot^2 \phi e^{2i\theta}$ under $z \mapsto w = z^2$. But since

$$|j_{\pm}(\theta) + 1| |j_{\pm}(\theta) - 1| = |\cot^2 \phi e^{2i\theta}| = \cot^2 \phi,$$

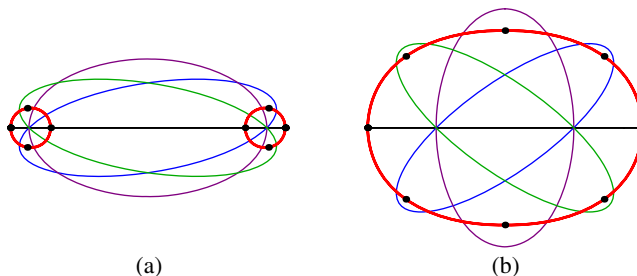


Figure 7 A $\pi/3$ -focus locus (a) and a $\pi/6$ -focus locus (b).

the focus locus is a Cassini oval with foci $z = \pm 1$ and eccentricity $\tan \phi$. As ϕ varies between 0 and $\pi/2$, the foci loci form the confocal family of Cassini ovals illustrated in Figure 1. When $\pi/4 < \phi < \pi/2$, the focus locus has two components, each traced by a focus winding about $z = \pm 1$ (Figure 7(a)). But when $\phi < \pi/4$, the foci wind about $z = 0$ and trace a continuous path (Figure 7(b)).

A solution of the focus locus problem

We now solve the focus locus problem from the introduction. Since the parallel projection $\Pi_{\phi, \theta}$ maps the center $(0, 0, 1)$ of \mathcal{C}^+ to the center $z = \cot \phi e^{i\theta}$ of the ellipse $\Pi_{\phi, \theta}(\mathcal{C}^+)$, (4) gives

$$z = h_{\pm}(\phi, \theta) = \cot \phi e^{i\theta} \pm \sqrt{1 + \cot^2 \phi e^{2i\theta}}, \quad 0 \leq \theta \leq 2\pi \quad (5)$$

as a parameterization of the ϕ -focus locus. Figures 8 and 9 show some of these foci loci. Now *each* locus has two components. The components are congruent when $\pi/4 \leq \phi < \pi/2$, but differ dramatically if $\phi < \pi/4$.

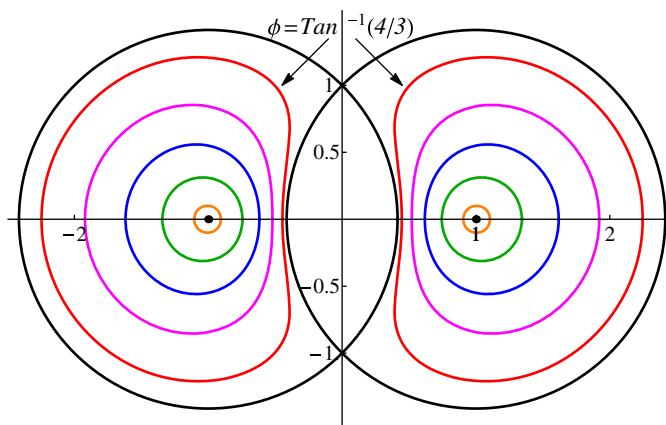


Figure 8 Some ϕ -foci loci, $\pi/4 \leq \phi \leq \pi/2$.

The $\pi/4$ -focus locus, the one that looks like a pair of circles (it is!) in both Figures 8 and 9, gives a subtle hint that the foci loci might be cross sections of tori. In 1848 Yvon Villarceau discovered that a bitangent plane, tangent to a torus at two points, cuts out a circle pair [3, p. 132] (Figure 10). The angle at which the circles intersect depends upon the shape of the torus, so we need to take some care in describing the $\pi/4$ -focus locus as a toric cross section. (The circles in the focus locus intersect orthogonally.)

In fact, each ϕ -focus locus in Figures 8 and 9 is a cross section of a torus \mathcal{T}_{ϕ} , with major and minor radii $R = \csc \phi$ and $r = \cot \phi$, respectively. The cross section is cut by a plane passing through the center of the torus that makes an angle of ϕ with its equator. Figure 11 shows an example. Here is an outline of a proof.

(a) An equation of \mathcal{T}_{ϕ} , centered at $(0, 0, 0)$ and symmetric about the z -axis, is

$$\left(\sqrt{x^2 + y^2} - \csc \phi\right)^2 + z^2 = \cot^2 \phi.$$

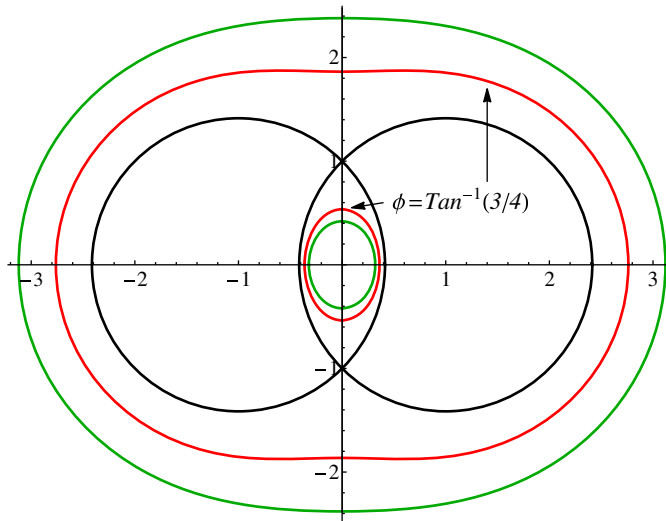


Figure 9 Some ϕ -foci loci, $0 < \phi \leq \pi/4$.

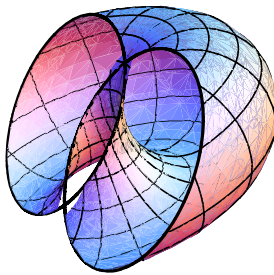


Figure 10 $T_{\pi/4}$ and a cross section, a $\pi/4$ -focus locus.

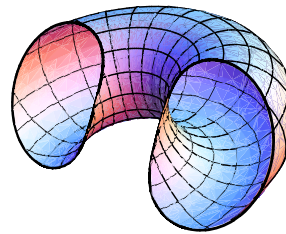


Figure 11 T_{ϕ} and a cross section, a ϕ -focus locus, $\phi = \tan^{-1}(4/3)$.

Rotate T_{ϕ} about the x -axis by the angle ϕ by substituting

$$(y \cos \phi - z \sin \phi, \quad y \sin \phi + z \cos \phi)$$

for (y, z) . Then substitute $z = 0$ to get

$$\sin^2 \phi (x^2 + y^2 + 1)^2 = 4(x^2 + y^2 \cos^2 \phi) \quad (6)$$

as an equation of the cross section.

- (b) To show (5) is equivalent to (6), first note that the focal points defined by (5) are the solutions to the quadratic equation

$$z^2 - 2z \cot \phi e^{i\theta} - 1 = 0. \quad (7)$$

Let $z = x + iy$ and equate the real and imaginary parts of (7). This gives

$$\begin{cases} x^2 - y^2 - 1 = 2(x \cos \theta - y \sin \theta) \cot \phi, \\ 2xy = 2(x \sin \theta + y \cos \theta) \cot \phi. \end{cases}$$

Square both sides and add to get

$$(x^2 - y^2 - 1)^2 + 4x^2 y^2 = 4(x^2 + y^2) \cot^2 \phi. \quad (8)$$

Some algebra shows that (8) is equivalent to (6), proving that any point of the focus locus (5) lies on the cross section (6).

- (c) To show, conversely, that any point of the cross section lies on the focus locus, let $z = x + iy$ and rewrite (8) as

$$|z^2 - 1| = 2|z| \cot \phi.$$

Then $z^2 - 1 = 2z \cot \phi e^{i\theta}$ for some $\theta \in [0, 2\pi)$ and $x + iy$ is a root of (7).

So the ϕ -foci loci generated by the unit circles \mathcal{C} and \mathcal{C}^+ are *both* cross sections of tori. The former is a Cassini oval with unit semifocal length and eccentricity $\tan \phi$. It is a spiric section of a torus with major and minor radii $R = 1$ and $r = (\cot^2 \phi)/2$, cut by a plane normal to its equator (See the comments in the introduction.) The latter is a cross section of the torus \mathcal{T}_ϕ , cut by a plane through its center and making the angle ϕ with the equator.

Further explorations

We end with some observations and suggestions for variations on the focus locus problem that the reader might enjoy exploring.

1. There is another way to describe the foci loci of Figures 8 and 9. We claim (Figure 12) that
 - (a) the image of each focus locus under stereographic projection is a pair of congruent spherical ellipses* on the Riemann sphere S^2 , and that
 - (b) the stereographic images of the ϕ -focus locus and the $(\pi/2 - \phi)$ -focus locus are congruent. A 90° rotation of S^2 about the y -axis swaps the two pairs of spherical ellipses.

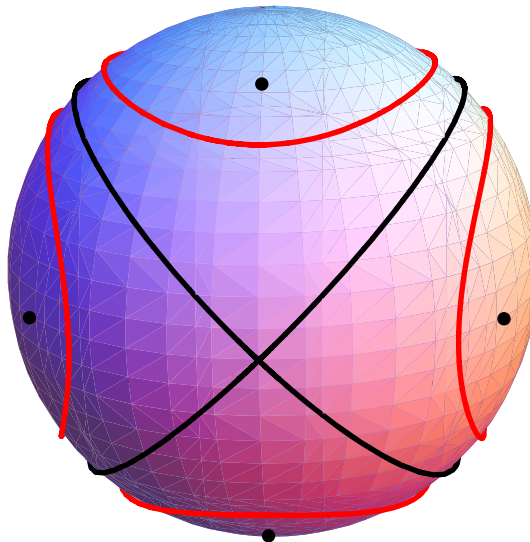


Figure 12 The stereographic images of the ϕ and $(\pi/2 - \phi)$ -foci loci, $\phi = \tan^{-1}(3/4)$. The great circle pair is the stereographic image of the $\pi/4$ -focus locus.

*A spherical ellipse is defined much like an ellipse in the plane, but distances are measured along arcs of great circles. It is the locus of points, the sum of whose *spherical distances* from two fixed points is constant.

It is not immediately obvious that each focus locus in Figure 9 maps to a pair of *congruent* curves on S^2 . The key point is to recognize that each ϕ -focus locus is invariant under the map $z \mapsto 1/\bar{z}$. (Each path is clearly invariant under $z \mapsto \bar{z}$ and $z \mapsto -z$, and by (7) also invariant under $z \mapsto -1/\bar{z}$.) This map, inversion in the unit circle, corresponds to a reflection of the Riemann sphere about the xy -plane. For an insightful introduction to these ideas and an explanation of how a rotation of the Riemann sphere gives rise to a Möbius transformation (useful in proving (b)), we recommend [5].

2. We can use ellipses to generate foci loci as well. While we do not recognize the ϕ -focus locus generated by a general origin-centered ellipse, there is one exception. Suppose we rotate the ellipse $\{(x, 0, z) \mid x^2/a^2 + z^2/b^2 = 1\}$ clockwise (as viewed from the positive y -axis looking toward the origin) by 45° about the y -axis. Then the $\pi/4$ -focus locus is the preimage of the curve

$$w = (a^2 - b^2 + (a^2 + b^2) \cos \theta) e^{i\theta}, \quad 0 \leq \theta \leq 2\pi \quad (9)$$

under $z \rightarrow w = z^2$. The curve (9) is a limaçon (from the Latin *limax*, for snail) with an inner loop, as in Figure 13. The preimage of *each* loop of the limaçon under the squaring map is a lemniscate and the focus locus is a lemniscate *pair* (Figure 14). When $a = b$, (9) defines a circle and the lemniscate pair collapses into two identical copies of Bernoulli's lemniscate.

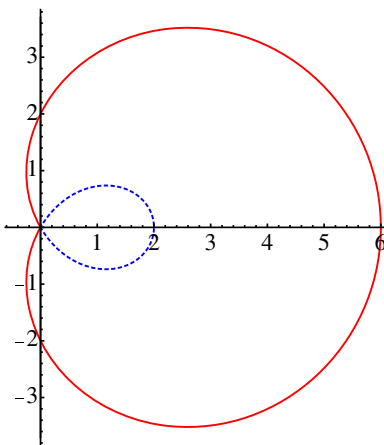


Figure 13 A limaçon (9), $a = \sqrt{3}$, $b = 1$.

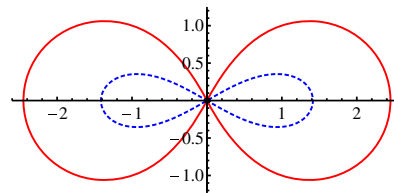


Figure 14 A lemniscate pair, the preimage of the limaçon in Figure 13 under the squaring map.

Acknowledgment We would like to thank the referees for their suggestions that narrowed the focus and improved the clarity of this paper.

REFERENCES

1. H. J. M. Boss, *Lectures in the History of Mathematics*. American Mathematical Society, Rhode Island, 1993.
2. E. Brieskorn, H. Knörrer, *Plane Algebraic Curves*. Birkhäuser, Basel, 1986.
3. H. S. M. Coxeter, *Introduction to Geometry*. Second edition. Wiley Classics Library, John Wiley and Sons, NJ, 1989.
4. J. C. Langer, D. A. Singer, When is a curve an octahedron?, *Amer. Math. Monthly* **117** (2010) 889–902.
5. T. Needham, *Visual Complex Analysis*. Clarendon Press, Oxford, 1998.
6. S. Northshield, Geometry of cubic polynomials, *Math. Mag.* **86** (2013) 136–143.

Summary. We investigate curves (foci loci) traced by the foci of one-parameter families of ellipses. The elliptical families are shadows cast by a circle. The focal paths turn out to be cross sections of tori.

MICHAEL GAUL (MR Author ID: [1125337](#)) received his MS in Mathematics at the University of Washington in 2007 under the direction of Yu Yuan. He's been teaching at North Seattle College for the past 6 years. In his spare time he enjoys traveling, playing music, reading, and watching movies.

FRED KUCZMARSKI (MR Author ID: [944646](#)) received his Ph.D. from the University of Washington under the guidance of Paul Goerss. He currently teaches at Shoreline Community College. In addition to thinking about mathematics, he enjoys baking bread and hiking in Washington's Cascades.

1	H	2	A	3	H	4	N		5	P	6	E	7	R	8	P	9	S		10	M	11	E	12	N	13	G																
14	I	M	A	Y		15	E	M	A	C	S		16	A	R	A	L		17	K	A	R	E	18	N	S	M	I	T	H		19	C	O	D	E							
20	E	N	D		21	U	T	I					22	B	A	S	I	N		23	T	24	I	M	O	T	25	H	26	Y	27	G	O	W	E	R	S						
28	A	29	B	O	M	B		30	T	E	S	L	A							31	B	I	G	A	S		32	S	E	A	T	33	T	34	L	35	E						
36	D	R	E	G		37	C	38	H	A	R	M		39	R	E	A	40	P		41	S	T	E	42	R	E	O	S		43	M	Y	A	S	S							
						44	A	L	O	H	45	A		46	E	M	P	T	Y		47	R	48	O	49	B	50	E	R	T	D	E	V	51	A	N	E	Y					
52	E	Z	R	A	S						53	A	M	S			54	E	55	X	56	P		57	R	O	O	T		58	C	59	O	60	L	I	N	A	61	D	A	M	S
62	A	N	N	I			63	O	B	E	L	I		64	O	R	E	S		65	N	E	X	T		66	G	E	S	S	O		67	I	S	N	T						

George Hart: Troubadour for Geometry*

AMY L. REIMANN

Ella Sharp Museum
Jackson, MI 49203
amyr@ellasharp.org

DAVID A. REIMANN

Albion College
Albion, MI 49224-1831
dreimann@albion.edu

George Hart is a sculptor, artist, mathematician, and one of the organizers of *Bridges: Mathematical Connections in Art, Music, and Science*, an annual, international conference. We sat down with George at Bridges Baltimore 2015 to discuss his background, philosophy of art, and artwork. A portion of this interview appears below. Accompanying artwork appears on the following pages: W, X, Y, and Z.

Q: *What's your educational background?*

GH: I have a mathematics degree from MIT as an undergraduate. I also have a Master's Degree in Linguistics where I studied formal language theory, what a computer needs to know to understand formal language, and the mathematics of language. I went back to MIT to work with Chomsky a little bit towards a Ph.D. in linguistics before changing my mind and deciding to pursue a Ph.D. in Electrical Engineering and Computer Science. None of that is directly related to sculpture.

Q: *What is your main occupation?*

GH: My main occupation is a troubadour for geometry. I go around the world letting people know geometry is wonderful by giving lectures, workshops, and making sculptures. Officially I'm a research professor at Stonybrook University, but that's sort of an honorary title. I'm not teaching so I am free to do whatever I like and this is what I like.

Q: *How long have you been creating art?*

GH: Since I was a kid, I can't really remember not making things that were geometric and sculptural in some sense. Things just got fancier over time.

Q: *What did you make things out of when you were a kid?*

GH: A lot of paper and origami sorts of things, but more like paper polyhedra; cutting things out, taping and gluing them. I remember making giant structures out of toothpicks and Duco Cement®, big geometric things. The smell of Duco Cement still flashes me back to that time. It dried fast. Before hot melt glue, it was the fastest glue I knew. I remember holding these toothpicks, one at a time, in small bunches until they solidified.

Q: *Do you have any formal art-based training or education?*

GH: I took a number of art history classes as an undergraduate. I took one welding course at a museum just outside of Boston when I was working at MIT. But that's really it. I've largely been self-taught with a lot of library work and museum visiting and studio work on how to make stuff. My art is very highly designed and engineering based. I'm assembling things. A lot of my engineering training was very good for art: problem solving, how to fix things, figuring things out, what parts go can together, and

Math. Mag.* **88 (2015) 374–376. doi:10.4169/math.mag.88.5.374. © Mathematical Association of America
MSC: Primary 01A70; Amy L. Reimann (MR Author ID: 1118776) and David A. Reimann (MR Author ID: 912704)



Millennium Bookball (left), George Hart; wood and bronze, 5 feet in diameter, 1999; Northport Public Library, Northport, NY.

Roads Untaken (right), George Hart; wood, 17 inches in diameter, 1999; private collection.

patience. Designing tools is another big aspect of engineering. Instead of just making the thing, first you make a tool that helps you make the thing. And that philosophy, I think, informs my art in a sense in which you see these complex sculptures I make but you don't see all the tools that I make first. Those are gone when you see the final art.

Q: *What mediums do you normally work in?*

GH: I work constructively in all different media. I've made sculptures out of pencils or CDs or all kinds of wood or books. I do a lot nowadays with metal or wood that's been laser-cut. The boring part is making all the components. The fun part is assembling them. So I can ship out to a laser-cutting company or I can laser-cut in my studio, instead of using a band saw or whatever. Cutting the pieces can be farmed out to a machine and so the fun parts of designing it and putting it together are left for me.

Q: *What are your inspirations?*

GH: Many, a great many. Martin Gardner's [writings] taught me about the enormous breadth of mathematics, that it's not just what you see in school. He really had a gift for teaching how to think like a mathematician, to not just believe in isolated facts, but see how they fit into a bigger pattern, how one leads to another. That lets you see a whole structure of things. And that way of thinking, which is the essence of mathematics, he really conveyed well to a general public better than anyone else I think. So he was a major inspiration and he also talked about art. In the art world, all kinds of sculpture inspired me. I think Calder and Picasso and other 20th century abstract sculpture just resonated with me. I enjoy the visual way of trying to understand things. There's always a puzzle when I look at a sculpture. Can I understand it if I shut my eyes or turn around? Can I see it entirely in my mind and challenge myself—yeah I get it; I could go to a desert island and reproduce that because I've got it internalized. I think that is a challenge I want people to try when they look at my sculpture—to see it deeply enough to understand how all the parts go together as one.

Q: *What work in the 2015 Bridges show surprised you?*

GH: Surprised me? Different sorts of things. I can tell you which one I bought. My partner Elisabeth and I, we bought a piece by David Chapelle, who makes beautiful



Loopy (left), George Hart; painted aluminum (five colors), 6 feet in diameter, 1999; private collection. Constructed of thirty woven loops bolted together.

Frabjous (right), George Hart; wood, 11 inches in diameter, 2003; private collection. Assembled from thirty identical S-shaped pieces.

flowing organic prints that are entirely algorithmic. So there's a computer program and I totally understand how this program works. I can see it in my mind. But he's designed it in a way that it makes lovely curves and has a sense of hand to it. There's a kind of shading and a gracefulness which is unique or rare among purely algorithmic work. It really has a flow to it that I like.

Q: *What's a favorite piece of yours that you've made?*

GH: There's one at the top of my web page called *Roads Untaken*. It's a wooden sphere, maybe almost half a meter in diameter, made of 902 pieces of wood. I first made a fiberglass sphere of that size and the parts go on it like a mosaic. It took me almost a month to make, when I was at the point that I was really deciding that I was an artist. Before that I was a professor who made art on evenings and weekends. Then there was a point where I was like, Oh wait a minute, I'm really a sculptor; that's my main thing. Being a professor pays the bills. Being a professor gives me people to have lunch with and friends. But in making *Roads Untaken* I accepted the label [of artist] for myself.

AMY L. REIMANN (MR Author ID: [1118776](#)) is the executive director of the Ella Sharp Museum in Jackson, Michigan. She received her B.A. in Art History from Albion College, an M.S.I. in Archives and Records Management from the University of Michigan, and the Certificate of Nonprofit Executive Leadership from the Indiana University School of Public and Environmental Affairs. She serves on the boards of the American Museum of Magic and the Jackson (MI) Rotary Club and is a peer reviewer for the American Alliance of Museums. She is an avid knitter.

DAVID A. REIMANN (MR Author ID: [912704](#)) is a professor of Mathematics and Computer Science at Albion College. He received a B.S. in Mathematics from the University of Toledo, an M.A. in Mathematics from Wayne State University, and a Ph.D. in Computer Science from Wayne State University. He enjoys researching and creating mathematical art. He is currently serving as the project manager for MoSAIC (a collaborative effort from the Bridges organization, MSRI, and the Simons Foundation), which organizes a series of interdisciplinary mini conferences and festivals on mathematical connections in science, art, industry, and culture, held at colleges and universities around the United States and abroad.

PROBLEMS

BERNARDO M. ÁBREGO, *Editor*

California State University, Northridge

Assistant Editors: SILVIA FERNÁNDEZ-MERCHANT, California State University, Northridge; JOSÉ A. GÓMEZ, Facultad de Ciencias, UNAM, México; EUGEN J. IONASCU, Columbus State University; ROGELIO VALDEZ, Facultad de Ciencias, UAEM, México; WILLIAM WATKINS, California State University, Northridge

Editor's note. This marks the last issue in which Bernardo Ábrego is serving as the Problems Editor. Bernardo's colleagues from California State University, Northridge Silvia Fernández-Merchant and William Watkins are also completing their time on the Problems editorial board. I thank all of them for their contributions to the MAGAZINE over the last six years and wish them good luck in their next pursuits. Eduardo Dueñez from the University of Texas at San Antonio will begin his tenure as Problems Editor with the February 2016 issue.

Michael A. Jones, *Editor*

Due to an editorial oversight, Problems 1976 and 1978 in the October 2015 issue were duplicates of Problems 1952 and 1954 that had appeared in the October 2014 issue. In addition, the statement of Problem 1976 contains the following misprint: The condition " $n \geq 2$ " should read " $n \geq 1$ ". We thank Rob Pratt for pointing out this misprint. We apologize for these mistakes, and welcome readers to submit their solutions to Problems 1976 and 1978 even if they had already submitted solutions to 1952 and 1954.

PROPOSALS

To be considered for publication, solutions should be received by May 1, 2016.

1981. *Proposed by Marcel Chirita, Bucharest, Romania.*

Let $n \geq 2$ be an integer and a a real number different from 0 and ± 1 . Determine the polynomials $p(x)$ with real coefficients that verify the relation

$$(a^2x^2 + 1)p(ax) = (a^{2n+2}x^2 + 1)p(x),$$

for all real numbers x .

Math. Mag. **88** (2015) 377–384. doi:10.4169/math.mag.88.5.377. © Mathematical Association of America

We invite readers to submit problems believed to be new and appealing to students and teachers of advanced undergraduate mathematics. Proposals must, in general, be accompanied by solutions and by any bibliographical information that will assist the editors and referees. A problem submitted as a Quickie should have an unexpected, succinct solution. Submitted problems should not be under consideration for publication elsewhere.

Solutions should be written in a style appropriate for this MAGAZINE.

Solutions and new proposals should be mailed electronically (ideally as a \LaTeX or pdf file) to Eduardo Dueñez, Incoming Problems Editor. Problem proposals should be mailed electronically to mathmagproblems@maa.org and solutions to problems (except Quickies) should be mailed electronically to mathmagsolutions@maa.org. All communications, written or electronic, should include on each page the reader's name, full address, and an e-mail address and/or FAX number.

1982. *Proposed by George Apostolopoulos, Messolonghi, Greece.*

The diagonals of a convex quadrilateral $ABCD$ intersect at a point O such that $OB > OD$, $OC > OA$, and $\text{Area}(\triangle OAB) + \text{Area}(\triangle OCD) = \text{Area}(\triangle OBC)$. Let M and N be the midpoints of the diagonals \overline{AC} and \overline{BD} , respectively. Prove that the lines AN and DM intersect at a point that lies on the side \overline{BC} .

1983. *Proposed by Prapanpong Pongsriam, Silpakorn University, Nakhon Pathom, Thailand.*

Let $y_1 = 0$ and $y_n = 1/(3 - y_{n-1})$ for all $n \geq 2$. Assume that $x_1 \notin \{y_n : n \in \mathbb{N}\}$ and define for $n \geq 2$,

$$x_n = 3 - \frac{1}{x_{n-1}}.$$

Prove that the sequence (x_n) converges.

1984. *Proposed by Timothy Hall, PQI Consulting, Cambridge, MA.*

Evaluate

$$\int_0^\infty \frac{\ln t}{t^2 - 1} dt.$$

1985. *Proposed by Brooke Tooles (student), Rutgers University, Piscataway, NJ.*

Alice and Bob play the following game. They first agree on a positive integer $n > 1$, called the *target number*, which remains fixed. Throughout, the state of the game is represented by an integer, which is initially 1. Players take turns with Alice going first. Each turn, a player names a prime factor of n , and the state of the game is multiplied by this prime. If a player manages to make the state of the game exactly equal to the target number, n , then that player wins. If the state of the game ever exceeds n , then the game is declared a draw. Determine for which values of n each player has a winning strategy, and for which values of n the game should end in a draw.

Quickies

Answers to the Quickies are on page 383.

Q1055. *Proposed by Alina Sîntămărian and Ovidiu Furdui, Technical University of Cluj-Napoca, Cluj-Napoca, Romania.*

Let $n \geq 1$ be an integer. Calculate

$$\int_0^1 \frac{\ln(1 + x + \cdots + x^{n-1})}{x} dx.$$

Q1056. *Proposed by Joseph Tonien, University of Wollongong, Wollongong, Australia.*

Find all integers n and m such that $2016n - 2015m$ is a perfect square.

Solutions

When n^{100} ends in 376**October 2014****1951.** *Proposed by Timothy Hall, PQI Consulting, Cambridge, MA.*Find all positive integers n for which the last three digits in base 10 of n^{100} are 376.*Solution by Darin Brown, San Joaquin Delta College, Stockton, CA.*

The last three digits in base 10 of n^{100} are 376 if and only if n is even and coprime to 5. These conditions are necessary, because if n is odd or a multiple of 5, then so is n^{100} . To show these conditions are sufficient, let $n = 2k$ be coprime to 5. Then $n^{100} = 2^3 \cdot (2^{97} \cdot k^{100})$ is divisible by 8, and $n^{100} = n^{\phi(125)} \equiv 1 \pmod{125}$ by Euler's theorem. Since 376 is divisible by 8, and $376 \equiv 1 \pmod{125}$, the Chinese remainder theorem implies that $n^{100} \equiv 376 \pmod{1000}$.

Also solved by Adnan Ali (India); Ashland University Problem Solving Group; Dionne Bailey, Elsie Campbell, and Charles Diminnie; Michel Bataille (France); Brian D. Beasley; Douglas Brown and John Zerger; Darin Brown; Paul Budney; Natalie Burns; Robert A. Calcaterra; Kyle Calderhead; Hongwei Chen; John Christopher; Tim Cross (United Kingdom); Joseph DiMuro; Robert L. Doucette; Collin Suzie Ellison, Juanicia Johnson, and Ashley Williams; Ashley Ernst and Matthew Golden; FAU Problem Solving Group; Dmitry Fleischman; Natacha Fontes-Merz; Daniel Fritze (Germany); Oliver Geupel (Germany); Michael Goldenberg and Mark Kaplan; Tanisha Graydon, Aaron Logan, and Chad Hicks; Jerrold W. Grossman; GWstat Problem Solving Group; Joel K. Haack; Russell Harmening; Eugene A. Herman; Hofstra University Problem Solvers; Iowa State University Undergraduate Problems Solving Group; David Johnson, Natalie McCandless, Emily Nail, and Spencer Orman; Harris Kwong; Elias Lampakis (Greece); Stephanie Lash; Kee-Wai Lau (China); Gordon S. Lessells (Ireland); Reiner Martin (Germany); Missouri State University Problem Solving Group; José Heber Nieto (Venezuela); Northwestern University Math Problem Solving Group; Ha Yun Park (Korea); Pittsburg State University Problem Solving Group; Henry Ricardo; Arthur J. Rosenthal; Courtney Sallings, Jennifer Hilderbrand, George Andrews, and Justin Smith; San Francisco University High School Creative Problem Solving Group; Achilleas Sinefakopoulos (Greece); Nicholas C. Singer; Skidmore College Problem Group; Seth Tonsor; Michael Vowe (Switzerland); Edward T. White; Timothy Woodcock; Michelle Zeng; and the proposer. There was one incomplete or incorrect submission.

A recursive sequence related to Egyptian fractions**October 2014****1952.** *Proposed by Ángel Plaza, Universidad de las Palmas de Gran Canaria, Las Palmas, Spain.*Let $\{a_n\}_{n \geq 1}$ be the sequence of real numbers defined by $a_1 = 3$ and for all $n \geq 1$, $a_{n+1} = \frac{1}{2}(a_n^2 + 1)$. Evaluate

$$\sum_{k=1}^{\infty} \frac{1}{1 + a_k}.$$

Solution by Robert L. Doucette, McNeese State University, Lake Charles, LA.

For any positive integer $n \geq 3$, $(n-1)^2 > 2$ implies that $(n^2+1)/2 > n+1$ and so $a_n > n$ implies that $a_{n+1} = (a_n^2+1)/2 > (n^2+1)/2 > n+1$. Since $a_1 = 3$, $a_2 = 5$,

and $a_3 = 13$, it follows by induction that $a_n > n$, for all positive integers n , and so $\lim_{n \rightarrow \infty} a_n = \infty$. Because

$$\frac{1}{a_n - 1} - \frac{1}{a_n + 1} = \frac{2}{a_n^2 - 1} = \frac{2}{(2a_{n+1} - 1) - 1} = \frac{1}{a_{n+1} - 1},$$

it follows that

$$\frac{1}{a_n + 1} = \frac{1}{a_n - 1} - \frac{1}{a_{n+1} - 1},$$

and so the given series is telescoping. Thus

$$\sum_{k=1}^{\infty} \frac{1}{1 + a_k} = \lim_{n \rightarrow \infty} \sum_{k=1}^n \frac{1}{1 + a_k} = \lim_{n \rightarrow \infty} \left(\frac{1}{a_1 - 1} - \frac{1}{a_{n+1} - 1} \right) = \frac{1}{a_1 - 1} - 0 = \frac{1}{2}.$$

Editor's Note. Many solvers noted that the sequence $\{a_n\}$ is related to Sylvester's sequence $\{s_n\}$ defined by $s_1 = 2$ and $s_{n+1} = s_n^2 - s_n + 1$. It verifies that $a_n = 2s_n - 1$. The first k terms of Sylvester's sequence correspond to the denominators of the closest possible underestimate of 1 by any k -term Egyptian fraction.

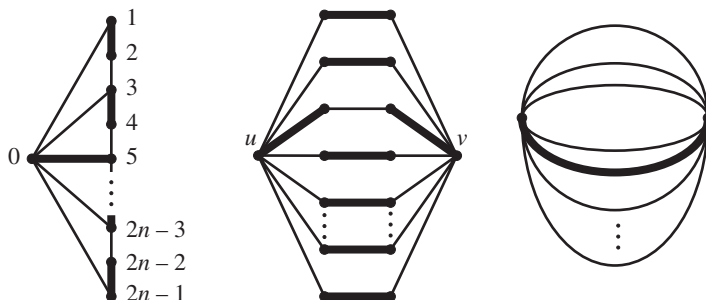
Also solved by Adnan Ali (India); Dionne Bailey, Elsie Campbell, and Charles Diminnie; Michel Bataille (France); Brian D. Beasley; Gerald E. Bilodeau; Brian Bradie; Darin Brown; Robert Calcaterra; Hongwei Chen; John Christopher; Tim Cross (United Kingdom); Prithwjit De (India); FAU Problem Solving Group; Daniel Fritze (Germany); Eugene A. Herman and Charles H. Jepsen; Hofstra University Problem Solvers; Brian Hogan; Michael Goldenberg and Mark Kaplan; Jerrold W. Grossman and László Lipták; Jaleb Jay; Harris Kwong; Stephanie Lash; Kee-Wai Lau (China); Gordon S Lessells (Ireland); James Magliano; Reiner Martin (Germany); Peter McPolin (Northern Ireland); Missouri State University Problem Solving Group; Northwestern University Math Problem Solving Group; Adrian Naco (Albania); José Heber Nieto; Moubinoöl Omarjee (France); Sungjun Park (Korea); Paolo Perfetti (Italy); Pittsburg State University Problem Solving Group; Rob Pratt; Henry Ricardo; Randy K. Schwartz; San Francisco University High School Creative Problem Solving Group; Achilleas Sinefakopoulos (Greece); Nicholas C. Singer; The University of Louisiana at Lafayette Math Club; Michael Vowe (Switzerland); Edward T. White; John T. Zerger; and the proposer. There were five incomplete or incorrect solutions.

Graphs with n perfect matchings

October 2014

1953. Proposed by Roberto Tauraso, Università di Roma "Tor Vergata," Roma, Italy.

Given a graph $G = (V, E)$, a *perfect matching* M of G is a subset of the set of edges E such that every vertex $v \in V$ lies on exactly one edge in M . Prove that for each positive integer n there is planar connected graph G whose total number of perfect matchings is equal to n .



I. *Solution by Oliver Geupel, Brühl, NRW, Germany.*

For any fixed positive integer n , let $V = \{0, 1, 2, \dots, 2n - 2, 2n - 1\}$ and

$$E = \{\{0, 2j - 1\} : 1 \leq j \leq n\} \cup \{\{j, j + 1\} : 1 \leq j \leq 2n - 2\}.$$

Consider the graph $G = (V, E)$ which is planar and connected. Let M be a perfect matching of G . Vertex 0 lies on exactly one edge in M , say on $\{0, 2k - 1\}$. Then the remaining edges in M are necessarily $\{2j - 1, 2j\}$, where $1 \leq j < k$ and $\{2j, 2j + 1\}$, where $k \leq j < n$. Since there are n possible choices of the number k , the total number of perfect matchings of G is n .

II. *Solution by Jerrold W. Grossman, Oakland University, Rochester, MI.*

Let G_n be the graph consisting of n disjoint paths of length 3 joining vertices u and v . This graph is clearly planar and connected. Any perfect matching of G_n must contain one edge incident to u , together with the edge on the same path of length 3 incident to v and the $n - 1$ edges on the other $n - 1$ paths incident to neither u nor v . There are clearly n such matchings.

III. *Solution by Ethan Gegner (student), Taylor University, Upland, IN.*

Fix a positive integer n , and let $G = (V, E)$ be the graph consisting of two vertices and n edges, with both vertices lying on all n edges. Then $M \subseteq E$ is a perfect matching of G if and only if $|M| = 1$. Thus, G has exactly n perfect matchings.

Editor's Note. Our solvers found a variety of families of graphs with the required property. FAU Problem Solving Group established that there are in fact infinitely many planar connected simple graphs with exactly n perfect matchings. The problem poser intended for the graphs to be simple, which would forbid the construction in the last solution. However, the construction can be modified to work for simple graphs, as shown by Grossman in the second solution.

Also solved by Robert A. Calcaterra, Eddie Cheng, Kyle Calderhead, Joseph DiMuro, Michael Dixon, Robert L. Doucette, FAU Problem Solving Group, Kenneth Fogarty, Natacha Fontes-Merz, Hofstra University Problem Solvers, Gordon S. Lessells, Reiner Martin (Germany), Missouri State University Problem Solving Group, Ángel Plaza (Spain), Rob Pratt, San Francisco High School Creative Problem Solving Group, John H. Smith, Michelle Zeng, and the proposer.

A limit of n -norm integrals

October 2014

1954. *Proposed by George Apostolopoulos, Messolonghi, Greece.*

Evaluate

$$\lim_{n \rightarrow \infty} \left(\int_1^{e^2} \left(\frac{\ln x}{x} \right)^n dx \right)^{1/n}.$$

Solution by Missouri State University Problem Solving Group, Missouri State University, Springfield, MO.

In general, if $f(x)$ is a nonnegative continuous function on $[a, b]$, it is well known that

$$\lim_{n \rightarrow \infty} \left(\int_a^b f(x)^n dx \right)^{1/n} = \max_{x \in [a, b]} f(x).$$

To see this, let $M = \max_{x \in [a, b]} f(x)$ and note that

$$\lim_{n \rightarrow \infty} \left(\int_a^b f(x)^n dx \right)^{1/n} \leq \lim_{n \rightarrow \infty} (M^n(b-a))^{1/n} = M.$$

On the other hand, because f is continuous, then for any $\varepsilon > 0$ there is a subinterval $[c, d]$ of $[a, b]$ such that $f(x) \geq M - \varepsilon$ for any $x \in [c, d]$. Therefore,

$$\begin{aligned} \lim_{n \rightarrow \infty} \left(\int_a^b f(x)^n dx \right)^{1/n} &\geq \lim_{n \rightarrow \infty} \left(\int_c^d f(x)^n dx \right)^{1/n} \\ &\geq \lim_{n \rightarrow \infty} ((M - \varepsilon)^n(d - c))^{1/n} = M - \varepsilon. \end{aligned}$$

Since ε is arbitrary, the result follows. In the given case, taking $f(x) = (\ln x)/x$ we have $M = 1/e$ when $x = e$. Therefore, the limit is $1/e$.

Editor's Note. Many of our solvers remarked that the more general result presented in the solution is well known. Some of the references given include Exercise 7.24 in T. Apostol, *Mathematical Analysis*, AddisonWesley, and Problem II.198 in George Pólya, Gabor Szegő, *Problems and theorems in analysis*, Springer-Verlag.

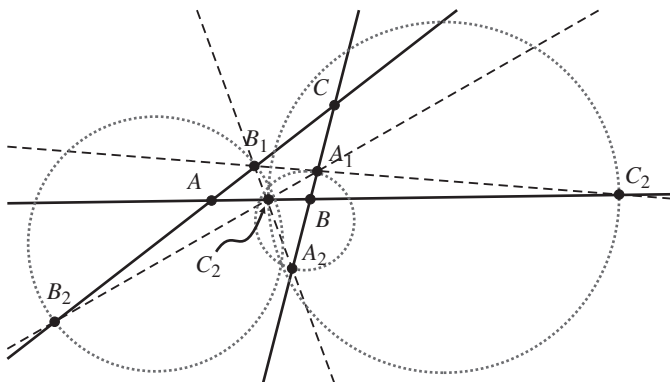
Also solved by Michel Bataille (France), Gerald E. Bilodeau, Brian Bradie, Darin Brown, Robert A. Calcaterra, Hongwei Chen, Bruce E. Davis, Robert L. Doucette, FAU Problem Solving Group, John N. Fitch, Daniel Fritze (Germany), Oliver Geupel (Germany), GWstat Problem Solving Group, Eugene A. Herman, Michael Goldenberg and Mark Kaplan, Hidefumi Katsuura, Elias Lampakis (Greece), Kee-Wai Lau (China), Andrew Markoe, Reiner Martin (Germany), José Heber Nieto (Venezuela), Northwestern University Math Problem Solving Group, Paolo Perfetti (Italy), Ángel Plaza (Spain), Henry Ricardo, Iason Rusodimos, Anna Seno and Allen Lunnies, San Francisco University High School Creative Problem Solving Group, Achilleas Sinefakopoulos (Greece), Nicholas C. Singer, Mritunjay Kumar Singh (India), Michael Vowe (Switzerland), and the proposer.

Intersection of Apollonian circles

October 2014

1955. Proposed by Elton Bojaxhiu, Kriftel, Germany and Enkel Hysnelaj, University of Technology, Sydney, Australia.

Let ABC be a triangle. Let A_1 , B_1 , and C_1 be points in the interior of \overline{BC} , \overline{CA} , and \overline{AB} , respectively, such that AA_1 , BB_1 , and CC_1 are concurrent. Let A_2 , B_2 , and C_2 be the respective points of intersection of the pairs of lines (B_1C_1, BC) , (C_1A_1, CA) , and (A_1B_1, AB) . Let P be a point in the plane. Show that if two of the angles $\angle A_1PA_2$, $\angle B_1PB_2$, and $\angle C_1PC_2$ are right angles, then the third angle must also be a right angle.



Solution by Achilleas Sinefakopoulos, M. N. Raptou Private High-School, Larissa, Greece.

Since $\overline{AA_1}$, $\overline{BB_1}$, and $\overline{CC_1}$ are concurrent, applying Ceva's theorem gives us

$$\frac{BA_1}{A_1C} \cdot \frac{CB_1}{B_1A} \cdot \frac{AC_1}{C_1B} = 1, \quad (1)$$

while applying the theorem of Menelaus to triangle ABC for the line $A_2C_1B_1$ (with unsigned distances) gives us

$$\frac{BA_2}{A_2C} \cdot \frac{CB_1}{B_1A} \cdot \frac{AC_1}{C_1B} = 1.$$

From these two relations it readily follows that $BA_1 : A_1C = BA_2 : A_2C$. Denote this common ratio by r_1 and note that the points A_1 and A_2 lie on the Apollonian circle ω_1 of diameter A_1A_2 , which is the locus of points P in the plane such that $BP : PC = r_1$. Working similarly we see that the points B_1 and B_2 lie on the Apollonian circle ω_2 of diameter B_1B_2 , which is the locus of points P in the plane such that

$$CP : PA = CB_1 : B_1A = CB_2 : B_2A := r_2,$$

while the points C_1 and C_2 lie on the Apollonian circle ω_3 of diameter C_1C_2 , which is the locus of points P in the plane such that

$$AP : PB = AC_1 : C_1B = AC_2 : C_2B := r_3.$$

A point P in the plane is such that two of the angles $\angle A_1PA_2$, $\angle B_1PB_2$, and $\angle C_1PC_2$ are right angles if, and only if, P belongs to the corresponding two of the circles ω_1 , ω_2 , and ω_3 . Equivalently, two of the following three ratios

$$BP : PC = r_1, \quad CP : PA = r_2, \quad \text{and} \quad AP : PB = r_3$$

hold true. ζ From equation (1) it follows that $r_1r_2r_3 = 1$, and so if any two of these ratios hold true, then so does the third, and hence P lies on all three circles ω_1 , ω_2 , and ω_3 . Accordingly, if any two of the angles $\angle A_1PA_2$, $\angle B_1PB_2$, and $\angle C_1PC_2$ are right angles, then so is the third one.

Also solved by Adnan Ali (India), Michel Bataille (France), Robert A. Calcaterra, Oliver Geupel (Germany), Michael Goldenberg and Mark Kaplan, Peter McPolin (Northern Ireland), Jerry Minkus, Adrian Naco (Albania), Titu Zvonaru and Neculai Stanciu (Romania), and the proposers.

Answers

Solutions to the Quickies from page 378.

A1055. The integral equals $(n-1)\pi^2/(6n)$. Note that

$$\begin{aligned} \int_0^1 \frac{\ln(1+x+\cdots+x^{n-1})}{x} dx &= \int_0^1 \frac{\ln((1-x^n)/(1-x))}{x} dx \\ &= \int_0^1 \frac{\ln(1-x^n)}{x} dx - \int_0^1 \frac{\ln(1-x)}{x} dx. \end{aligned}$$

Letting $t = x^n$ on the first integral and using the fact that $\ln(1 - t) = -\sum_{k=1}^{\infty} t^k/k$ for $0 \leq t < 1$, we have that

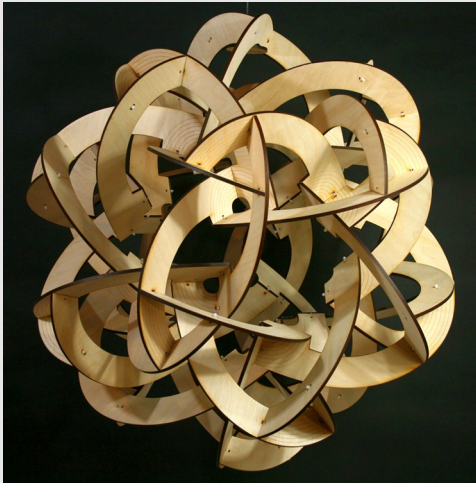
$$\begin{aligned} \int_0^1 \frac{\ln(1 + x + \cdots + x^{n-1})}{x} dx &= \left(\frac{1}{n} - 1\right) \int_0^1 \frac{\ln(1 - t)}{t} dt \\ &= \left(1 - \frac{1}{n}\right) \int_0^1 \sum_{k=1}^{\infty} \frac{t^{k-1}}{k} dt \\ &= \left(1 - \frac{1}{n}\right) \sum_{k=1}^{\infty} \frac{1}{k^2} = \frac{(n-1)\pi^2}{6n}. \end{aligned}$$

A1056. Let $2016n - 2015m = k^2$, then $n = k^2 + 2015(m - n)$. Let $a = m - n$, then $n = k^2 + 2015a$ and $m = a + n = k^2 + 2016a$. Therefore, $(n, m) = (k^2 + 2015a, k^2 + 2016a)$, where a and k are arbitrary integers.

New Year Identity

$$\left\lfloor \frac{{}^{2017}\sqrt{2015^{2015}} + {}^{2015}\sqrt{2017^{2017}}}{2} \right\rfloor = 2016$$

—Joseph Tonien, University of Wollongong



Artist Spotlight George Hart

Celebration of Mind, George Hart; wood, 30 inches in diameter, 2013; Fine Hall, Princeton University, Princeton, NJ. Constructed from 60 identical components made from 6-mm-thick birch plywood connected using cable ties.

See interview on page 374.

REVIEWS

PAUL J. CAMPBELL, *Editor*
Beloit College

Assistant Editor: Eric S. Rosenthal, West Orange, NJ. Articles, books, and other materials are selected for this section to call attention to interesting mathematical exposition that occurs outside the mainstream of mathematics literature. Readers are invited to suggest items for review to the editors.

Gamwell, Lynn, *Mathematics and Art: A Cultural History*, Princeton University Press, 2016; xx + 556 pp, \$49.50. ISBN 978-0-691-16528-8.

This review will not reach you in time for the 2015 winter holiday season, when this book could have been a gift for the coffee table. But it belongs on your coffee table, and it should stay there a long time—not because of its weight (at 7 lbs, it will stay where you put it)—but because this absolutely extraordinary book needs to be absorbed in small doses since *every page rewards with delight* (even the endpapers). The book is about art inspired by mathematics, e.g., by the ideas of infinity. A better description is that the book narrates and exhibits the “cultural impact of mathematical thought,” largely on art—it is a marriage of metamathematics and meta-art. The narration compares philosophies of mathematics with the practices of mathematics as set against the tensions between “rationalist accounts of the natural world” and humanistic-based rebellions against those visions. The exhibition is a gallery of an astonishing and imaginative variety of reproductions of ancient and contemporary art. Along the way, the author agrees to an interpretation of ancient Chinese mathematics as generalization without abstraction, debunks claims that ancient and other artists and architects used the “golden section” ($\phi = \frac{1}{2}(1 + \sqrt{5})$) as an ideal proportion for humans or buildings, investigates the origins of abstraction and the influence of computers in art, and concludes with a discussion of platonism in the postmodern era. “Today mathematics continues to inspire great art because abstract objects are, as Plato said, ‘eternally and absolutely beautiful.’” (On p. 53, “dual” should be “duel”; on p. 148, Figure 3-35, “rhombus-shaped” would be better as “square bifrustum-shaped”; and on p. 156, “non-Cantorian” should mean at least one transfinite number between \aleph_0 and the continuum.)

Wilkes, Jason, *Burn Math Class and Reinvent Mathematics for Yourself*, Basic Books, 2016; iv + 390 pp, \$28.99(P). ISBN 978-0-465-05373-5.

In the first sentence of the preface, the author backs away from the title’s invitation to burn down the school, insisting instead that he means only “conceptual arson”: He wants you to pretend that mathematics has not been invented, that it is not “a pre-existing subject that was created without you,” dumped on you to memorize. He begins with “machines” that “eat numbers and spit out other numbers” (i.e., functions), proceeds to model area as a function of length and width (applying bilinearity to the function $A(\ell, w)$), and goes on to model “steepness” of a line, and, later, of a curve. Calculus, too, gets invented, with the help of an “infinite magnifying glass” and “tinies” (infinitesimals). Later chapters derive various rules for differentiation, and “invent” the trigonometric functions and inverses and find their derivatives. Investigation of “machines” that turn addition into multiplication ($f(x + y) = f(x)f(y)$) and vice versa ($g(xy) = g(x) + g(y)$) leads to exponential and logarithmic functions. Integration and its relation to differentiation come into play, together with the formula for arc length. There are even “cannibalistic machines,” “which eat an entire machine and spit out a number” (i.e., functionals). The irreverence is useful (though some of the playful dialogues drag), and the approach *ex nihilo* is utterly refreshing.

Math. Mag. **88** (2015) 385–386. doi:10.4169/math.mag.88.5.385. © Mathematical Association of America

Castelvecchi, Davide, Paradox at the heart of mathematics makes physics problem unanswerable, *Nature* (09 December 2015) <http://www.nature.com/news/paradox-at-the-heart-of-mathematics-makes-physics-problem-unanswerable-1.18983>, doi:10.1038/nature.2015.18983.

Cubitt, Toby S., David Perez-Garcia, and Michael M. Wolf, Undecidability of the spectral gap, *Nature* 528 (10 December 2015) 207–211, doi:10.1038/nature16059.

The spectral gap of a physical system is the gap in energy level of its electrons between its ground state and its first “excited” state. Does a system have to have a gap? Cubitt et al. prove that the answer is in general algorithmically undecidable and also independent of the axiomatization of mathematics. Apart from the curiosity (a metamathematical result from theoretical physics), there is a connection to a Clay Millennium Prize Problem, the Yang–Mills mass-gap problem: Why/how could it be that particles that carry nuclear forces have mass but photons (which carry gravity and electromagnetism) don’t? The work of Cubitt et al. suggests that the Yang–Mills mass-gap problem too may be undecidable.

Mutalik, Pradeep, The road less traveled: When there are two paths to your destination, why does it always seem like you’re on the road with more traffic?, *Quanta Magazine* (September 3, 2015) <http://www.quantamagazine.org/20150903-the-road-less-traveled>.

The author cites selection bias as an explanation (the more crowded road has more drivers to sample from), tries to estimate the extent of the bias, and solicits comments (worth reading). The situation is analogous to the difference between the average number of students per class as recorded by the registrar (total students divided by total classes) and the larger average experienced by students (because more students are in larger classes).

Tawalkar, Presh, The hot hand is real?! Understanding a controversial statistics paper ..., <http://mindyourdecisions.com/blog/2015/10/06/the-hot-hand-is-real-understanding-a-controversial-statistics-paper-game-theory-tuesdays/>.

Gelman, Andrew, Hey—guess what? There really is a hot hand! [with comments], <http://andrewgelman.com/2015/07/09/hey-guess-what-there-really-is-a-hot-hand/>.

Miller, Joshua Benjamin, and Adam Sanjurjo, Surprised by the gambler’s and hot hand fallacies? A truth in the law of small numbers, <http://www.datascienceassn.org/sites/default/files/Surprised%20by%20the%20Gambler's%20and%20Hot%20Hand%20Fallacies%20A%20Truth%20in%20the%20Law%20of%20Small%20Numbers.pdf>.

Rinott, Yosef, and Maya Bar-Hillel, Comments on a “hot hand” paper by Miller and Sanjurjo (2015), <http://pluto.huji.ac.il/~rinott/publications/hothand14.pdf>.

Previous papers investigating streakiness and the “hot hand” phenomenon in sports compared the frequencies in data of “successes” (of basketball shots, etc.) with the probabilities predicted by the binomial model of independent trials. Miller and Sanjurjo note that those papers fail to condition the probabilities correctly. Tawalkar discusses the result in terms of biased estimation resulting from selection bias and gives a complete example for four coin flips, while Rinott and Bar-Hillel try to give a simplified explanation. The upshot is that the bias may mask a hot hand; that is, reanalysis of previous data may indeed give evidence for the hot hand phenomenon.

Roberts, Siobhan, New Erdős paper solves Egyptian fraction problem, (10 December 2015) <https://www.simonsfoundation.org/uncategorized/new-erdos-paper-solves-egyptian-fraction-problem/>.

Butler, Steve, Paul Erdős, and Ron Graham, Egyptian fractions with each denominator having three distinct prime divisors, http://www.math.ucsd.edu/~ronspubs/pre_tres_egyptian.pdf.

Twenty years after his death, Paul Erdős is still publishing, this time jointly with Steve Butler (Iowa State) and Ron Graham (UC–San Diego): Any natural number can be expressed as a sum of distinct unit fractions where each denominator is the product of three distinct odd primes. Can the result be improved to two distinct primes? You’ll have to wait for Erdős’s next paper.

ACKNOWLEDGMENTS

In addition to our Associate Editors, the following referees have assisted the MAGAZINE during the past year (May 2014 to May 2015). We thank them for their time and care.

Francine Abeles, *Kean University*
Jim Albert, *Bowling Green State University*
Bruce Bates, *University of Wollongong*,
Matthias Beck, *San Francisco State University*
Ethan Bolker, *University of Massachusetts Boston*
Michael Bolt, *Calvin College*
Neil Calkin, *Clemson University*
Dan Daly, *Southeast Missouri State University*
William Dunham, *Muhlenberg College*
Steven Edwards, *Southern Polytechnic State University*
Jerry Grossman, *Oakland University*
Michael Huber, *Muhlenberg College*
Thomas Hull, *Western New England College*
Yukio Kobayashi, *Soka University*
Dimitrios Kodokostas, *National Technological Institute of Athens*
Nikolai Krylov, *Siena College*
Milan Lukic, *American Mathematical Society*
Susan Marshall, *Monmouth University*
John McCleary, *Vassar College*
Francis Papp, *University of Michigan*
Timothy Pennings, *Davenport University*
Marc Renault, *Shippensburg University*
Bruce Reznick, *University of Illinois at Urbana-Champaign*
V. Rickey, *United States Military Academy*
Kenneth Ross, *University of Oregon*
Jessica Sklar, *Pacific Lutheran University*
Peter Turner, *Clarkson University*



MAA MATHFEST

August 3-6, 2016

Columbus, Ohio

Save the Date

Earle Raymond Hedrick Lectures

Hendrik Lenstra, University of Leiden

AMS-MAA Joint Invited Address

Ravi Vakil, Stanford University

MAA Invited Addresses

Arthur Benjamin, Harvey Mudd College

Judy Holdener, Kenyon College

Robert Megginson, University of Michigan

MAA James R. C. Leitzel Lecture

Annalisa Crannell, Franklin & Marshall College

AWM-MAA Etta Z. Falconer Lecture

Izabella Laba, University of British Columbia

MAA Chan Stanek Lecture for Students

Colin Adams, Williams College

Pi Mu Epsilon J. Sutherland Frame Lecture

Robin Wilson, Open University

NAM David Blackwell Lecture

Robert C. Hampshire, University
of Michigan Transportation
Research Institute

**Check our website for
registration and housing
information.**



Mathematical Association of America • maa.org/mathfest

CONTENTS

ARTICLES

- 323 How to Make the Perfect Fireworks Display: Two Strategies for *Hanabi* by Christopher Cox, Jessica De Silva, Philip DeOrsey, Franklin H. J. Kenter, Troy Retter, and Josh Tobin
- 337 Proof Without Words: Half Issues in the Equilateral Triangle and Fair Pizza Sharing by Grégoire Nicollier
- 338 How to Divide Things Fairly by Steven J. Brams, D. Marc Kilgour, and Christian Klamler
- 349 Volume/Surface Area Ratios for Globes, with Applications by Tom M. Apostol and Mamikon A. Mnatsakanian
- 360 The Parallelogram with Maximum Perimeter for Given Diagonals Is the Rhombus—A Proof Without Words and a Corollary by Angel Plaza
- 362 Crossword Puzzle: Joint Mathematics Meetings 2016 by Brendan W. Sullivan
- 364 The Focus Locus Problem and Toric Sections by Michael Gaul and Fred Kuczmarski
- 374 George Hart: Troubadour for Geometry by Amy L. Reimann and David A. Reimann

PROBLEMS AND SOLUTIONS

- 377 Proposals, 1981-1985
- 378 Quickies, 1055-1056
- 379 Solutions, 1951-1955
- 383 Answers, 1055-1056

REVIEWS

- 385 *Math's effects on art; burn math class!; the hot hand is hot; system gaps*

NEWS AND LETTERS

- 387 Acknowledgments